2021

Control Effect of Peracetic Acid on Chlorinated DBP Formation and the Application of PAA Pre-oxidation in Drinking Water Treatment

Yue Sun
University of Massachusetts Amherst

Control Effect of Peracetic Acid on Chlorinated DBP Formation and the Application of PAA Pre-oxidation in Drinking Water Treatment

A Masters Project Presented

by

YUE SUN

Approved as to style and content by:

DocuSigned by:
David Reckhow
235E2D4E373F49E...
David Reckhow, Chairperson

DocuSigned by:
John E. Tobiason
E74AD5B712444E7...
John Tobiason, Member

DocuSigned by:
01D6091B23DA416...
Caitlyn Butler
Civil and Environmental Engineering Department

Abstract

Chlorine has been applied as the main disinfectant in US drinking water treatment for a century. Chlorination is low cost and effective, yet there are problems with this technology, including disagreeable taste of treated drinking water and formation of toxic and potentially carcinogenic disinfection byproducts (DBPs). Alternative disinfection methods including ozone, ferrate and UV light have been studied. They are not widely applied in drinking water treatment because of problems such as the costly generation process or no residual in the system.

Peracetic acid, an easy-to-use and economic friendly oxidant, has been applied as an alternative disinfectant to chlorine in wastewater treatment. However, the study and application of PAA in drinking water treatment is limited. In this research, PAA disinfection and its use to control DBP formation during subsequent chlorination was examined. Different PAA operation scenarios were tested: disinfection in the dark at 20 °C with contact times up to 72 hours, decay under direct sunlight up to 18 hours and decay in the dark at 20 °C with different short contact times. Best DBP control effect was observed in the 72-hour PAA pre-oxidation test. Direct sunlight accelerated PAA decomposition and shown higher ability to drop the amount of DBPs formed during subsequent chlorination. Among the scenarios tested in this study, the optimum disinfection condition for PAA was 2 hours of PAA pre-disinfection in the dark at 20 °C.

Keywords: disinfection byproduct; peracetic acid; DBP control; kinetics

Content

1 Introduction

The alternative disinfectants to chlorine have been widely explored since the discovery of halogenated disinfection byproducts. Chlorine dioxide, ozone, ultraviolet irradiation, peracids have been studied and compared. Peracetic acid (PAA), a member of the organic peracid family, has drawn attention in the water industry recently because of its benefits including strong oxidizing ability, low byproduct formation and low operational cost. PAA is a strong oxidant with a wide spectrum of microbial inactivation. PAA has its highest oxidation potential when in neutral form. The high pKa (8.2) ensures the stability of the neutral form of PAA in even a slightly alkaline matrix. These properties make PAA competitive in wastewater disinfection. The advanced oxidation processes (AOPs) application of UV/PAA and PAA with catalyst metals were widely studied in micropollutant treatment and sludge solubilization. PAA generates reactive oxidizing species (ROS) when activated by UV irradiation or catalyst. The constituent removal efficiency of activated PAA is much higher than PAA alone, and even higher than UV/H_2O_2 in some cases.

PAA has been applied as a disinfectant in food industry, pulp bleaching and wastewater treatment. But the application of PAA in drinking water treatment is rare. The objective of this study is to test the DBP control ability of PAA pre-oxidation in drinking water. PAA decomposition processes in the dark and under sunlight were observed and the decay kinetics were modeled. These and other factors affecting bench-scale process performance were explored.

2 Alternative Disinfectants

For decades, chlorine has been the dominant disinfectant in drinking water and wastewater treatment. However, the formation of disinfection byproducts has raised concerns over chlorine's use since the 1970s. More and more studies have revealed that DBPs are toxic, carcinogenic, mutagenic and teratogenic. DBPs are not only a threat to human health but also to the aquatic ecosystem. The concerns over DBPs have motivated the investigation of alternative disinfection methods to traditional chlorination.

2.1 Comparison of Different Disinfectants

Different alternative disinfection methods have been studied, and applied in practice, including ultraviolet radiation (UV), ozone and organic peracids such as PAA. For E.Coli treatment at typical Ct values (the product of concentration of disinfectant and time), UV was proved to have higher disinfection efficiency than ozone, PAA and hypochlorite. UV resulted in nearly 100% inactivation of E coli and coliforms in a few seconds with a dose of 10-20 mJ/cm^2. Ozone was proved to require the lowest dose and contact time to achieve a 4-5 logarithmic inactivation of E.coli and coliforms

(Luukkonen et al., 2017). PAA was the least efficient disinfection method compare to ozone and UV, but it iscomparable to hypochlorite.

However, the release of hazardous ozone gas needs to be controlled. UV absorbance is highly sensitive to the physical-chemical characteristics of the matrix. Compared to chemical alternatives like PAA and peroxide, UV treatment and ozonation are relatively complex techniques that require expensive equipment and tedious maintenance thus much higher investment cost for similar treatment efficiency as PAA. The implementation of techniques like UV and ozonation can require substantial capital improvement which may take a long time (Henao et al., 2018). The operational cost, investment cost and total cost (figure 1) of PAA, ozone, UV and ClO_2 were calculated by Collivignarelli et al. in 2000. The total cost of ozonation is higher than PAA disinfection. The energy consumption of UV irradiation is higher than PAA operation.

The application of organic peracids (R-COOOH) in wastewater treatment is attracting more and more attention. The common beneficial features of peracids are their effective anti-microbial properties, lack of harmful disinfection byproducts and high oxidation power (Luukkonen et al., 2015). However, peracid disinfection in surface water and groundwater treatment has been barely studied.

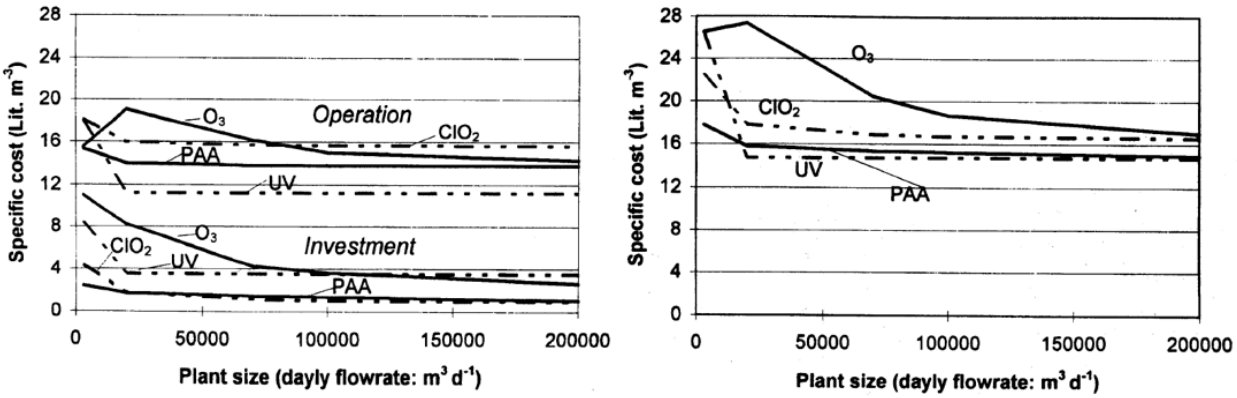

Figure 1. Investment, operation and total cost of UV, ozone, PAA and chlorine dioxide for different sizes of treatment plants. Costs were expressed in Itatian Lira (1 US $ = 1,700 Lit. by then). Adapted from Colivignarelli et al., 2000.

2.2 Peracids

The organic peracids typically present as an equilibrium solution containing peracid, hydrogen peroxide, the corresponding carboxylic acid and water (equation (1)) (Luukkonen et al., 2015). Additionally, small amounts of catalysts or stabilizers can be present.

$$R\text{-}COOOH\ (aq) + H_2O\ (l) = R\text{-}COOH\ (aq) + H_2O_2\ (aq) \quad (1)$$

Performic acid (PFA) and PAA are industrially the most relevant peracid because of their high oxidation potential. They have the potential to replace several other industrial biocides that have undesirable properties, such as formaldehyde, bromine or isothiazoline (Luukkonen et al., 2017). They have many qualities of an ideal disinfectant, such as, toxicity to microorganisms but little or no toxicity to higher forms of life; stability and long shelf life; low corrosivity; widespread availability and reasonable cost. The concentrations of PAA and PFA in commercial equilibrium solutions are typically 5-15% and 8-13.5% as the active ingredient respectively (Ragazzo, P et al., 2013 and Tondera, K., 2016). The operational costs of disinfection were estimated to be 0.0114 and 0.0261 Euro/m^3 for PFA and PAA (Luukkonen et al., 2017).

However, PFA is unstable and needs to be prepared on-site shortly before use (Mattila and Aksela, 2000). There are potential safety issues in the process due to the explosive nature of PFA at elevated temperatures and concentrations. PFA has been shown to be especially effective in disinfecting primary wastewater effluents (Gehr et al., 2009) and combined sewer overflows (Chhetri et al., 2015, 2014). However, PFA's disinfection effectiveness in drinking water treatment needs to be tested partly because PFA is known to undergo rapid and non-selective reactions.

PAA has one additional methyl carbon than PFA, which gives it greater chemical stability. As a result, PAA can be stored and supplied as a ready-to-use liquid. Furthermore, PAA has been shown to have similar beneficial features to PFA, such as lack of harmful DBPs under typically applied conditions and no significant re-growth of bacteria occurring after disinfection (Antonelli et al., 2006). Therefore, PAA is an especially interesting peracid for water disinfection.

3 PAA

PAA was first prepared as a disinfectant in 1900s (Freer and Novy, 1902). The application of PAA in environmental sanitation was first described in 1970s. USEPA registered PAA as an anti-microbial agent in 1985. Since then PAA has been intensively studied. The behavior of PAA in wastewater treatment from different sources has been evaluated (Koivunen et al., 2005b; West et al., 2016) and mathematical models have been developed for its use (Manoli et al., 2019). In addition to its potential for disinfection, researchers have studied the kinetics of PAA decomposition (Zhang et al. (2018); Zhao et al. (2007); Yuan and Van Heiningen (1997)), byproduct formation (Monarca et al. (2004); Crebelli et al. (2005); Dell'erba et al. (2007); Xue et al. (2017)), and ecotoxicity (Henao et al. (2018); Macedo et al. (2019)). Theoretical studies were also conducted to demonstrate the molecular structure (da Silva et al., 2020) and thermodynamic properties of PAA (Zhang et al., 2018) to explain experimental observations and to further predict the disinfection behavior of PAA. The application of

PAA in advanced oxidation processes has also been explored. The most promising combinations include UV/PAA, Fe/PAA, and Co/PAA.

3.1 physicochemical characteristics (disinfection efficiency)

PAA is a colorless liquid with a vinegar-like odor, a high boiling point (100°C) and a low melting point (0.2°C). It has relatively high pKa value (8.2) compared to other organic acids, which allows PAA to represent as neutral form even in slightly alkaline environment. PAA is a stronger oxidant in neutral form than anion form, and this property has been taken advantage of in wastewater treatment (Kim et al., 2019).

The Lewis acid structure of PAA simulated by Zhang et al. (2018) (figure 2) indicates that each of the three oxygen atoms are in different oxidation states. The standard redox potentials of PAA are 1.748 V and 1.005 V vs. standard hydrogen electrode (SHE) at pH 0 and pH 14, respectively. Under biochemical standard state conditions (pH 7, 25 °C, 101,325 Pa), PAA has a redox potential of1.385 V vs. SHE. This is higher than many disinfectants, including H_2O_2 (1.349 V), hypochlorous acid (1.288 V), chlorine dioxide (1.168 V), chloramines (1.098 V), and hypobromous acid (1.134 V).

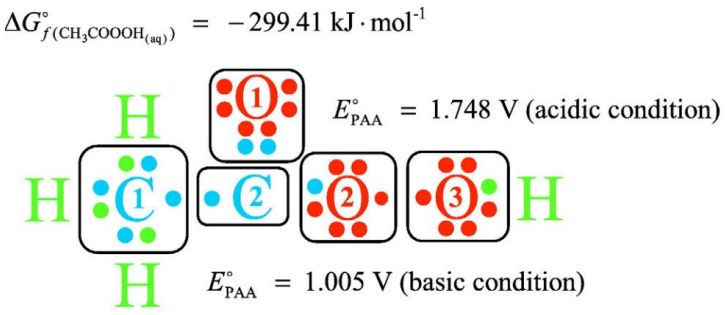

Figure 2. The Lewis structure of PAA. Adapted from Zhang et al., 2018.

3.2 molecular structure

Figure 3 displays the molecular structures of PAA and H_2O_2 as simulated by da Silva et al. (2020). PAA may generate hydroxyl radicals (·OH) from the O-O bond in a similar way as H_2O_2. The O-O bond of PAA (1.443 Å) is similar as and slightly longer than the O-O bond of H_2O_2 (1.427 Å). The energy required to break the O-O bond of PAA (38 kcal mol^{-1}) was shown to be lower than that of peroxide (51 kcal mol^{-1}) (Bianchini et al., 2002). The topological analysis revealed the electron density of O-O bonds in PAA and H_2O_2 are 0.284922 au and 0.297995 au, respectively. These all show that the O-O

bond of H_2O_2 is stronger than that of PAA. This implies that PAA is reactive than H_2O_2 in AOPs since the formation of ·OH are preferred at lower energy demand.

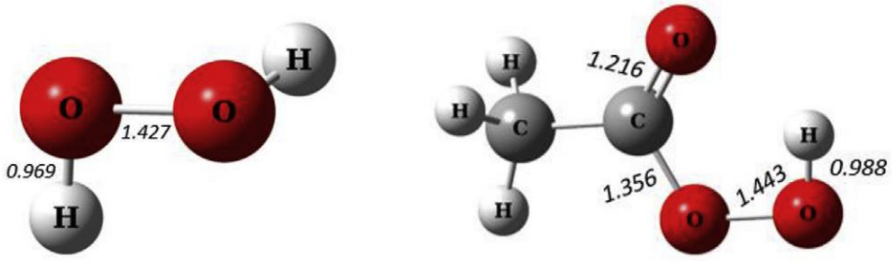

Figure 3. Bond lengths for H_2O_2 and PAA, data in Å. Adapted from da Silva et al., 2020.

The formation of the intramolecular H-bond, resulting in the rotation angles of the CO-OH presents a proximity of the hydrogen of hydroxyl with the oxygen of the carbonyl, contributing to the stability of the neutral form of PAA(da Silva et al., 2020). The weak acid behavior of PAA avoids the need for pH adjustment after application.

3.3 decomposition mechanism

Two separate decomposition mechanisms for PAA were proposed by da Silva et al. (2020) depending on the pH; one for pHs below 5.5 and another for pHs between 5.5 and 10.2. When pH is below 5.5 (figure 4.1), PAA decomposition occurs in three steps: protonation, formation of a PAA dimer (active intermediate) and decomposition of the dimer yielding the final products. There were three possible ways of protonation: a) the carbonyl oxygen; b) the peroxy oxygen and c) hydroxy oxygen. It was concluded that site a) is the most likely of the three (Carey, 2011). After protonation, the molecule reorganized to form a carbocation on the central carbon and reacts as a Lewis acid in the mechanism. Then another PAA molecule attacks the carbocation, resulting in formation of an active dimeric intermediate and release of protons. In the last step, the intermediate decomposes into two acetic acid molecules and one oxygen molecule. The relative energy value between the attack step and the final product was 22 kcal mol^{-1}, implying that the decomposition is spontaneous. The formation of acetic acid of PAA decomposition justified the BOD or TOC increase after PAA disinfection. Thus, BOD or COD are not recommended as a monitoring parameter for disinfection processes with PAA.

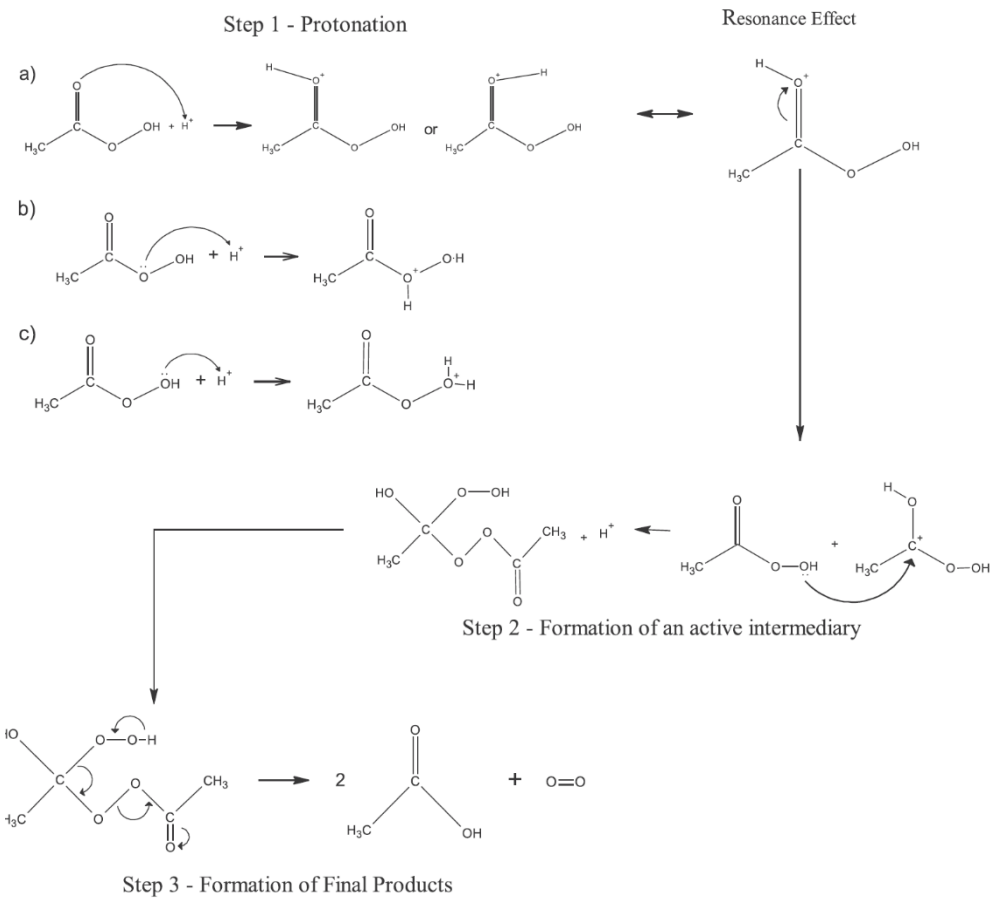

figure 4.1 Spontaneous decomposition of PAA in acetic acid and O_2 at pH < 5.5. Adapted from da Silva et al., 2020.

When pH is between 5.5-10.2 (figure 4.2), PAA decomposition occurs in two steps: attack of peracetic anion on PAA and formation of deprotonated dimeric active intermediate, and decomposition of the intermediate into acetate anions, O_2 and H^+ products. This mechanism is supported by observations in this study at UMass and by the studies of Chen and Pavlostathis (2019) and Pedersen et al. (2009), where the decomposition rate increased with higher concentrations of PAA in the treated effluent**.** High concentration of PAA favors this mechanism which the PAA molecules react with each other and promoted the decomposition process. At low concentration the decomposition slows down, and PAA is able to maintain effective CT levels to inhibit microbial growth.

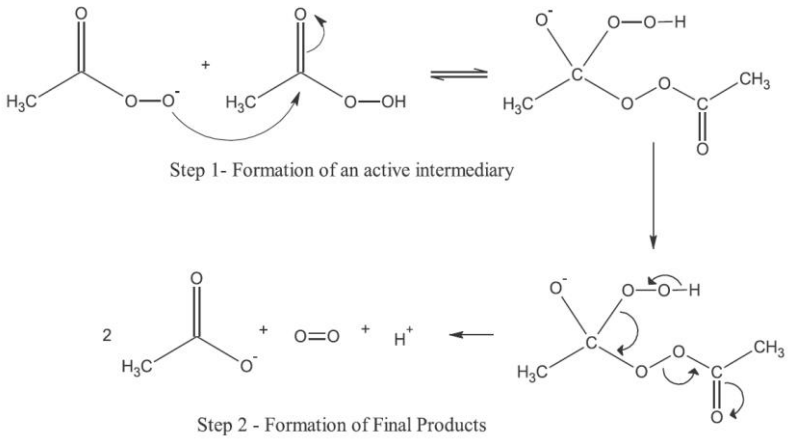

Figure 4.2 Spontaneous decomposition of PAA in the pH range of 5.5-10.2. Adapted from da Silva et al., 2020.

The process of PAA decomposition in dilute acidic medium (figure 4.3) is similar to the acidic mechanism already presented, except that the attacking species is water instead of another PAA molecule. The mechanism can be divided into five steps: protonation and formation of the carbocation, attack of water molecule on the intermediate, followed by three subsequent protonation or deprotonation steps resulting in the formation of acetic acid and hydrogen peroxide. The energy difference between the protonation and the formation of acetic acid and H_2O_2 is low, which means an equilibrium is established corresponding to the stability of the compound. The results agree with the commercial composition of PAA, which is a quaternary equilibrium of H_2O_2, PAA, acetic acid and water (equation 1).

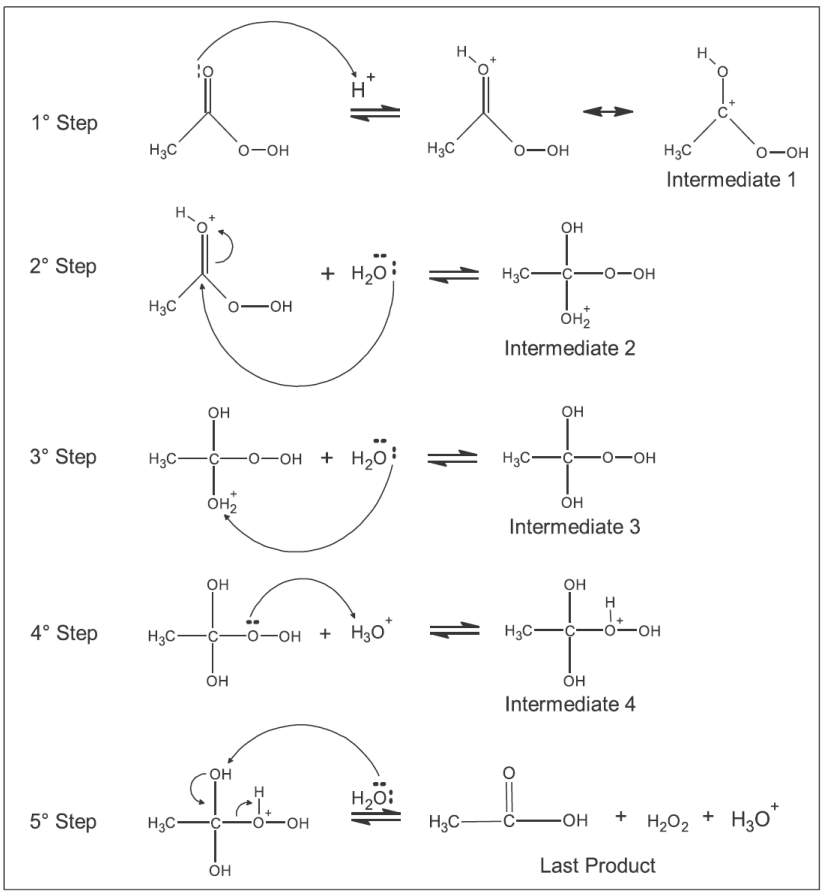

Fig. 6. Hydrolysis of PAA in acidic medium.

Figure 4.3 Hydrolysis of PAA in acidic medium. Adapted from da Silva et al., 2020.

3.4 Decay Kinetics

Based on de Silva's mechanism and assuming the rate limiting step is attack on the carbocation, the kinetics of decay for PAA should be second order in PAA at high concentrations, and first order at low concentrations. The observed decay of PAA in wastewater has been modeled as a zero – order decay (Santoro et al., 2007) with 0.993 R^2 and a first – order decay (Falsanisi et al., 2006; Rossi et al., 2007) with 0.992 R^2. In both cases, the first order rate constant of PAA has varied from 0.0028 – 0.0396 min^{-1} in different matrices. These correspond to half-lives of from 0.5 to 4 hours (i.e., 29 and 248 min). Luukkonen et al. (2015) reported the modeling of PAA decay in tap water with an initial dose of 15ppm. The rate constants for zero-order, first-order and second-order modeling were 0.0159, 0.0009 min^{-1} and 0.00007 $mM^{-1}min^{-1}$ separately with R^2 of 0.972, 0.970 and 0.962.

The half – lives (t_{50}) of PAA in different kinds of matrix have been studied and summarized in table 1. T_{50} was reported between 18 – 710 min with the shortest times reported in primary effluent and

longest in potable water (Luukkonen et al, 2015). T_{50} of tap water was reported to be 100 min by Rossi et al. in 2007 and estimated to be in the range of 469 – 710 min by Luukkonen et al. in 2015. The Half-lives (T_{50}) of PAA treated (1-15 ppm) secondary effluents ranges from 77 to 248 min (Cavallini et al., 2013; Dell'Erba et al., 2004; Falsanisi et al., 2006; Rossi et al., 2007). T_{50} of tertiary effluents treated with 15 ppm PAA ranges from 168-189 min (Luukkonen et al., 2015). T_{50} of PAA (1-5ppm) in aquaculture systems reported by Pedersen et al. (2009) ranged from 36-318 min depending on the organic matter content and PAA concentration.

Dilute solutions of hydrogen peroxide are generally considered stable at 20°C in distilled water free from light and catalytic surfaces. However, even small amounts of transition metals and particles can cause measurable rates of decomposition, forming water and molecular oxygen. Thus, the lifetime for hydrogen peroxide in water is entirely dependent on the dissolved and particular matter present. For example, the t_{50} for H_2O_2 in a surface water has been measured at 264, 282, 384, 1146 and 3522 min in unfiltered, 64 mm filtered (zooplankton removed), 12 mm filtered (large algae removed), 1 mm filtered (small algae removed) and 0.2 mm filtered (bacteria removed) samples, respectively (Cooper et al., 1994). In comparison to hydrogen peroxide, PAA decay kinetics in surface water have been little studied, but from existing data it is clear that PAA is the less stable and more reactive of the two.

Table 1. Half-Lives of PAA in Different Matrices

Matrix	PAA dose (mg/L)	T_{50}, PAA (min)	pH	UV254	TOC	BOD	COD	DO	TSS	biomass	reference
Tap water	1-15	100	7.46	0.018	-	-	-	-	-	-	Luukkonen, 2015
Tertiary effluent	15	168-189	7.41	0.398	-	2.35	53.4	-	391	-	Luukkonen, 2015
Wastewater	1-15	77-248	6.2-7.8	0.205-0.241	-	-	43-365	3.6-5.8	8.8-96	-	Cavallini et al., 2013; Falsanisi et al., 2006; Rossi et al., 2007
Surface ater, decay in dark	0.5-1.5	192-624	6.5-7.2	0.088	2.88	-	-	-	-	-	This study
Surface water, decay under sunlight	0.5-1.5	192-252	6.5-7.2	0.05	2.2	-	-	-	-	-	This study
Aquaculture systems	1-5	36-318	-	-	-	-	-	-	-	24 kg/m3	Pedersen, 2009

3.5 Analytical method

Most common methods for PAA are non-specific and either spectrophotometric or titrametric. Sully et al. (1962) developed an iodometric method whereby liberated iodine is titrated with thiosulphate and using starch as an endpoint indicator. Another method relies on N, N-diethyl-p-phenylenediamine (DPD – $(C_2H_5)_2C_6H_4NH_2$) oxidation with the free radical product determined by

cerimetric/iodometric titration and permanganometric/iodometric titration depending on the PAA concentration range. A spectrophotometric method using DPD and catalase was recommended for 0.1 – 0.5 mg/L PAA concentrations and the cerimetric/iodometric titration or the DPD method were suitable for 0.5–10 mg/L PAA. The iodometric titration with the catalase addition could be used between 1 and 5 mg/L PAA, whereas the permanganometric/iodometric titration was not recommended at all (Cavallini et al., 2013).

A DPD method was modified for accurate measurement of PAA in order to avoid problems caused by spontaneous decay of the analyte. Zhang et al. (2020) compared three methods: spectrophotometric total chlorine reagent (SPTCR) method (namely solid DPD method), solution DPD and iodine/thiosulphate titration. The SPTCR method was shown to be the most accurate and precise method among the three. Titration is the least accurate one because of operational errors. The SPTCR method was used in this study with HACH pocket colorimeter.

PAA can also be measured online by reagent-free optical biosensors. This method is based on the determination of absorption of intermediate compounds resulting from a reaction between peroxidase and H_2O_2 or PAA (Sanz et al., 2007).

3.6 PAA vs H_2O_2

As PAA always exists in equilibrium with hydrogen peroxide the use of PAA solutions really invokes the simultaneous reaction of both oxidants. Various studies showed the superiority of the disinfection/oxidation potential of PAA in relation to hydrogen peroxide (Aslari et al., 1992; Lubello et al., 2002; Kitis, 2004 and Du et al., 2018). PAA equilibrium solutions produced higher levels of disinfection than hydrogen peroxide alone. Hydrogen peroxide was found to require much higher doses than PAA for the same level of disinfection (Wagner et al., 2002).

The performance of PAA vs H_2O_2combined with activators (resulting in AOPs) has been widely studied. C. Lubello et al. (2002) investigated the disinfection efficacy of UV/PAA and UV/H_2O_2 on secondary wastewater effluent on pilot scale. High disinfection performance is necessary to meet Italy's strict limit on unrestricted wastewater reuse in agriculture (2 CFU Total Coliform /100mL). Both PAA and H_2O_2 were shown to be satisfactory and the log removal reached 4.4 – 5.5 with addition of UV irradiation. At a cost parity, PAA showed better performance than H_2O_2 and the UV/PAA AOP exhibited the same performance as UV/H_2O_2. While at a cost and dose parity, UV/PAA was more effective than UV/H_2O_2. Hollman et al. (2020) compared the removal efficiency of UV/PAA and UV/H_2O_2 on the emerging substances of concerns (ESOCs). Under similar conditions, UV/H_2O_2 was found to be faster than UVC/PAA to degrade venlafaxine (VEN), carbamazepine (CBZ), fluoxetine (FLU) while UVC/PAA was faster on sulfamethoxazole (SFX) degradation.

In both PAA and H_2O_2 AOPs, higher doses resulted in better constituent removal. But it is important to determine the optimum dose of PAA or H_2O_2 to avoid the scavenging effect of hydroxyl radicals (Rizzo et al., 2018; Hollman et al., 2020). PAA was shown to have a strong scavenging effect on ·OH under high PAA concentration or alkaline (PAA- dominant) conditions (Cai et al., 2017). Hydrogen peroxide could also dissociate into HO_2^- and both HO_2^- and ·OH could react subsequently with H_2O_2. The possible reactions of radicals were shown below (equation 2.1-2.5). The subsequent reactions of H_2O_2 with the intermediate of UV/H_2O_2 could cause a scenario whereby high H_2O_2 doses accelerate ·OH consumption by H_2O_2 other than target compounds.

$$H_2O_2 + h\nu \rightarrow 2\,HO^{\cdot} \quad (2.1)$$

$$H_2O_2 \rightarrow H^+ + HO_2^- \quad (2.2)$$

$$HO^{\cdot} + H_2O_2 \rightarrow HO_2^{\cdot} + H_2O \quad (2.3)$$

$$HO_2^{\cdot} + H_2O_2 \rightarrow HO^{\cdot} + H_2O + O_2 \quad (2.4)$$

$$HO^{\cdot} + HO_2^- \rightarrow O_2^- + H_2O \quad (2.5)$$

Adapted from Hollman et al., 2019.

PAA can also serve as an acetyl of substitution for hydrogen peroxide in Fenton processes. The H_2O_2- based Fenton process is a green treatment method with a wide range of applications including drinking water contaminant oxidation, purification of treatment plant residuals, and sludge conditioning. However, the preference for acidic (pH<4) conditions raises the cost of the technique. PAA can reduce the electron cloud density of the H_2O_2 bond atom and is more prone to dissociation, so PAA is more oxidative and acidic than H_2O_2 (Wang et al., 2015 in Chinese). This makes PAA an interesting substitute for peroxide.

4 PAA AOPs

The oxidation of contaminants by peroxides is often accomplished by the reactive oxygen species (ROS) formed as a result of peroxide decomposition, including hydroxyl radical (HO·), the superoxide anion (·$O2^-$), the hydroperoxyl radical (HO_2^-), acyl and per acyl radicals. The radical formation is enhanced in advanced oxidation processes.

The possible radical formation pathways of PAA are presented in equations 3.1-3.7 (Luukkonen et al., 2017). The first step (equ. 3.1) requires activation by UV irradiation or metal catalysts, and it is the rate-determining step in the overall reaction sequence. Hydroxyl radicals are considered the dominant ROS for the degradation of a wide range of organic compounds by AOPs (e.g., Cai et al., 2017; Du et al., 2018). Hollman et al. (2020) confirmed the importance of ·OH radicals by identifying the degradation intermediates, which coincided with all the byproducts generated during UV/H_2O_2 process. The carbon-centered radicals formed during the AOPs, especially CH_3·, CH_3CO·, CH_3COO·, and CH_3COOO·, are important in the disinfection process since the carbon-centered radicals are more selective and have longer half-lifes than HO· (Cai et al., 2017; Hollman et al., 2020). It was also suggested that the hydrocarbon component (e.g., methyl group) of PAA could help the radicals penetrate microbial cells (Koivunen and Heinonen–Tanski, 2005).

$$CH_3COOOH \rightarrow CH_3COO\cdot + HO \quad (3.1)$$
$$CH_3COOOH + HO\cdot \rightarrow CH_3CO\cdot + O_2 + H_2O \quad (3.2)$$
$$CH_3COOOH + HO\cdot \rightarrow CH_3COOO\cdot + H_2O \quad (3.3)$$
$$CH_3COO\cdot \rightarrow \cdot CH_3 + CO_2 \quad (3.4)$$
$$2CH_3COO\cdot \rightarrow 2\cdot CH_3\cdot + 2CO + O_2 \quad (3.5)$$
$$\cdot CH_3 + O_2 \rightarrow CH_3OO\cdot \quad (3.6)$$
$$CH_3COO\cdot + HO\cdot \rightarrow CH_3COOOH \quad (3.7)$$

Possible Pathways of Radical Formation from PAA by AOPs, adapted from Luukkonen et al. (2017)

4.1 UV/PAA

It was shown that UV irradiation could effectively activate PAA to form ROS and the UVC portion of the spectrum is more effective than UVA. Pharmaceuticals were persistent with PAA alone but degraded rapidly by the combination of UVC (254nm) and PAA (Cai et al., 2017). UV light increased the inactivation rate of antibiotic resistant E.coli by low concentrations of PAA in both groundwater and wastewater. And the rate was higher with UVC irradiation than with solar light, which is mainly UVA (Rizzo et al., 2018). UVC with PAA resulted in degradation of emerging substances of concerns (ESOC) including VEN, CBZ, FLU and SFX while the UVA/PAA combination was not effective on most of the ESOCs in the test of Hollman et al. (2020).

The disinfection efficacy of PAA with UV irradiation was validated in a 5-month pilot scale test by Caretti and Lubello (2003). The effluent was not capable of meeting Italian legislations with either UV or PAA alone. However, the disinfection efficacy was enhanced with UV+PAA and further improved with PAA+UV treatment. This suggests that the formation of free radicals from PAA by UV

activation was the main reason of disinfection efficiency improvement. The possible pathways of ROS formation by UV/PAA is shown below (equ. 4.1-4.6). The initial reaction of PAA under appropriate UV irradiation is the cleavage of the oxygen double bond, leading to the generation of an acetyloxyl radical ($CH_3C(=O)-O$) and a hydroxyl radical (Cai et al., 2017; Caretti and Lubello, 2003) (Equation (4.1)):

$$CH_3CO_3H + h\nu \rightarrow CH_3CO_2^{\cdot} + HO^{\cdot} \qquad (4.1)$$

If unreacted, the acetyloxyl radical will dissociate to form a methyl radical and carbon dioxide (equ. 4.2)

$$CH_3CO_2^{\cdot} \rightarrow {}^{\cdot}CH_3 + CO_2 \qquad (4.2)$$

The methyl radical may then combine with dissolved oxygen to form a weak methyl peroxy radical (equ. 4.3)

$${}^{\cdot}CH_3 + O_2 \rightarrow CH_3OO^{\cdot} \qquad (4.3)$$

Similar to H_2O_2, HO• can react with PAA, creating a limiting reaction that removes HO• from solution while producing less reactive acetylperoxyl radicals (equ. 4.4-4.5)

$$CH_3CO_3H + HO^{\cdot} \rightarrow CH_3CO^{\cdot} + O_2 + H_2O \qquad (4.4)$$

or

$$CH_3CO_3H + HO^{\cdot} \rightarrow CH_3CO_2H^{\cdot} + HOO^{\cdot} \qquad (4.5)$$

Acetyloxyl radicals may also react with PAA in solution to produce acetylperoxyl radicals (equ. 4.6)

$$CH_3CO_3H + CH_3CO_2^{\cdot} \rightarrow CH_3CO_3^{\cdot} + CH_3CO_2H \qquad (4.6)$$

Possible Pathways of Radical Formation from UV/PAA, adapted from Hollman et al., 2020

The effluent was able to meet the Italian regulation for wastewater agricultural reuse (maximum concentration of 2 MPN/100 ml Total Coliforms for unrestricted irrigation), with 2 ppm of PAA and 192 mJ/cm^2 UV irradiation at a cost of 0.031 $Euro/m^3$ (Caretti and Lubello, 2003). The combination of low

dose of PAA and low intensity of UV irradiation was also shown to be cost-effective by the Metropolitan Sewer District (MSD) of Greater Cincinnati during their full-scale plant-level pilot test with UV/PAA on secondary effluent for six months. Pre-treatment with low doses of PAA increased the rate of microbial inactivation during UV irradiation. Pre-treatment with low doses of PAA (<2.0 ppm) and 20-23 min contact time followed by UV (41 and 89 mJ/cm^2) reduced the geometric mean of fecal coliform and E.coli to below 200 and 126 CFU/100mL respectively. At the effective PAA doses 2.0 and 0.75 ppm, the PAA residual in the effluent was below 1.0ppm. As a result, there is no need to quench the PAA residuals before discharging the water unless the Ohio EPA set a specific discharge limit. With the low cost and easy-to-install PAA pre-disinfection, the treatment plant was able to achieve cost savings by decreasing the UV intensity, power usage and the maintenance cost.

4.2 PAA Activation by Catalyst

The combination of PAA and catalysts, such as activated carbon fibers and metal ions, is also effective in water and wastewater pre-treatment. Zhou et al. (2015) reported the minor contribution of •OH in the removal of red dye in a PAA/activated carbon fiber system. Manganese dioxide (MnO_2) was used with PAA along with UV irradiation and this was shown to be effective at degrading phenol (Rokhina et al., 2013).

Several researchers have examined the use of iron with PAA for water and wastewater treatment. Ferrous iron (Fe^{+2}) was found to accelerate the biodegradation of organic substances when combined with PAA treatment. Iron combined with PAA caused degradation in the cell envelope, degradation in extracellular polymeric substance (EPS) and acceleration of the sludge solubilization process (Wang et al., 2020). PAA was also shown to have a positive effect on sludge anaerobic digestion and dewatering performance (Zhang et al., 2016; Sun et al., 2018).

The combination of Iron and PAA (Fe/PAA) was also shown to be effective at removing emerging micropollutants. PAA reacted with Fe^{2+} much more rapidly than H_2O_2 and it outperformed the accompanying H_2O_2 for degrading methylene blue (MB), naproxen (NPX), and bisphenol-A (BPA) (Kim et al., 2019). The possible pathways of radical generation were hypothesized as equ 5.1-5.5, which may generate primary RS such as $CH_3C(O)O$•, •OH, and $Fe(IV)O^{2+}$. Ferric iron (Fe(III)), generated from oxidation of Fe(II), can also react with H_2O_2 to generate superoxide radical (equ 5.6 and 5.7). Further reactions (equ 5.8-5.15) of primary RS, such as $CH_3C(O)O$•, •OH, and $Fe(IV)O^{2+}$ with PAA and H_2O_2 may occur and generate secondary RS, such as $CH_3C(O)OO$•,$CH_3(C)O$•, and HO_2•. The ferryl oxide species (Fe(IV)O2+) also reacts with water to form •OH (equ 5.16). The PAA radical ($CH_3C(O)O$•) can also rapidly self-decay to •CH_3 and CO_2 (equ 5.17), and the methyl radical can combine with oxygen to

produce a weak peroxyl radical $CH_3OO\bullet$ (eq 5.18).

$$CH_3C(O)OOH + Fe^{2+} \rightarrow CH_3C(O)O^{\bullet} + Fe^{3+} + OH^{-} \quad (5.1)$$

$$CH_3C(O)OOH + Fe^{2+} \rightarrow CH_3C(O)O^{-} + Fe^{3+} + {}^{\bullet}OH \quad (5.2)$$

$$CH_3C(O)OOH + Fe^{2+} \rightarrow CH_3C(O)OH + Fe^{IV}O^{2+} \quad (5.3)$$

$$H_2O_2 + Fe^{2+} \rightarrow {}^{\bullet}OH + Fe^{3+} + OH^{-} \quad (5.4)$$

$$H_2O_2 + Fe^{2+} \rightarrow H_2O + Fe^{IV}O^{2+} \quad (5.5)$$

$$H_2O_2 + Fe(III) \rightarrow HO_2^{\bullet} + Fe(II) + H^{+} \quad (5.6)$$

$$CH_3C(O)OOH + Fe(III) \rightarrow CH_3C(O)OO^{\bullet} + Fe(II) + H^{+} \quad (5.7)$$

$$CH_3C(O)OOH + CH_3C(O)O^{\bullet} \rightarrow CH_3C(O)OO^{\bullet} + CH_3C(O)OH \quad (5.8)$$

$$H_2O_2 + CH_3C(O)O^{\bullet} \rightarrow HO_2^{\bullet} + CH_3C(O)OH \quad (5.9)$$

$$CH_3C(O)OOH + {}^{\bullet}OH \rightarrow CH_3C(O)OO^{\bullet} + H_2O \quad (5.10)$$

$$CH_3C(O)OOH + {}^{\bullet}OH \rightarrow CH_3C(O)^{\bullet} + H_2O + O \quad (5.11)$$

$$CH_3C(O)OOH + {}^{\bullet}OH \rightarrow CH_3C(O)OH + HO_2^{\bullet} \quad (5.12)$$

$$H_2O_2 + {}^{\bullet}OH \rightarrow HO_2^{\bullet} + H_2O \quad (5.13)$$

$$H_2O_2 + 2Fe^{IV}O^{2+} \rightarrow HO_2^{\bullet} + Fe^{3+} + OH^{-} \quad (5.14)$$

$$CH_3C(O)OOH + 2Fe^{IV}O^{2+} \rightarrow CH_3C(O)O^{-} + 2Fe^{3+} + OH^{-} + O_2 \quad (5.15)$$

$$Fe^{IV}O^{2+} + H_2O \rightarrow {}^{\bullet}OH + Fe^{3+} + OH^{-} \quad (5.16)$$

$$CH_3C(O)O^{\bullet} \rightarrow {}^{\bullet}CH_3 + CO_2 \quad (5.17)$$

$${}^{\bullet}CH_3 + O_2 \rightarrow CH_3OO^{\bullet} \quad (5.18)$$

Adapted from Kim et al., 2019.

Cobalt (Co) is considered a highly-efficient catalyst for the acceleration of PAA decomposition, and one that is much more efficient compared to some other transition metals such as manganese, iron and copper (Zhang et al., 1998). PAA or Co alone barely removed the micropollutant sulfamethoxazole

(SMX) while the combination of PAA/Co degraded SMX rapidly. The H_2O_2 in the PAA are confirmed not to count for the removal of SMX (Wang et al., 2020). Co is more aggressive than Fe or copper in depleting PAA (Zhang et al., 1998). Co is widespread in surface water and groundwater at the concentration level of 1-10 μg/L (Smith and Carson, 1981; Hamilton, 1994), and widely detected in soils and sediments (Kim et al., 2006). Such concentration in natural environment is at the same level applied in the Co/ PAA process. Therefore, the Co/PAA process might also have potential application for the in situ chemical remediation of contaminated waters and soils without addition of Co (Wang et al, 2020).

5 PAA Application

5.1 global application

PAA has been used widely as a disinfectant in various industries such as food and beverage processing, brewery, pharmaceutical, pulp and paper, as well as medical applications, water in cooling systems and water treatment(Block, 1991; European Chemicals Agency, 2015; Malchesky, 2008). The largest user is the food industry. PAA was applied as a disinfectant in fresh produce washing water, clean-in-place processes, on food processing equipment, and in pasteurizers. The largest users of PAA on a global scale are shown in figure 5 (Luukkonen et al., 2017).

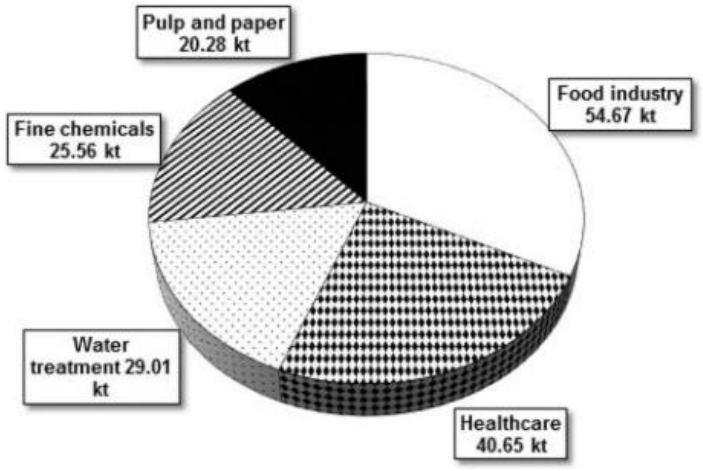

Figure 5 . The largest user segments of PAA in 2013 on a global scale. Adapted from Luukkonen et al., 2017.

5.2 cost

PAA is an expensive disinfectant (0.75 € kg^{-1}, 1999) even if the price if decreasing with the increasing market demand (Nurizzo et al., 2001). The cost of PAA in Europe is about US$ 3/gal (US$ 0.80/L) for 12% PAA by weight solution, which is approximately 4 – 5 times the cost of sodium hypochlorite. In 2002, the cost of PAA was roughly 4 times that of H_2O_2 (Lubello et al., 2002). The cost of PAA based disinfection (4 – 14 mg/L, 30 min contact time, tertiary wastewater effluent) has been estimated to be 0.048-0.098 €/m^3 depending on the required microbial quality (Nurizzo et al., 2001). Stabilized PAA chemical price was estimated at 1100 – 1200 €/ton and the operational cost was 0.0261 €/m^3 with 3.0 mg/L dose. The cost of PAA disinfection per amount of treated municipal wastewater has been estimated to be 0.0200–0.0645 €/m^3 (Luukkonen et al., 2015; Liberti and Notarnicola, 1999; Nurizzo et al., 2001; Koivunen et al., 2005). The investment costs of PAA systems (e.g.,dosing equipment, and contact tanks) are estimated to be 0.015–4.4 M€ (3000–200 000 m^3/d capacity plants) (Luukkonen et al., 2015; Colliviganarelli et al., 2000). In another study, the investment costs of a PAA system (including equipment, construction, electricity, automation, and overheads) were estimated to be 0.4 M€ for a 24 000 m^3/d capacity plant with an additional annual investment cost of 0.052 M€ (Koivenen et al., 2005).

Among PAA, UV, hypochlorite and ozone, the total cost of PAA was the highest (Nurrizo et al., 2001). In the pilot scale test conducted by Nurrizo et al. (2001), the cost percentage increments due to the additional disinfection with PAA, UV, NaOCl and ozone were compared. PAA was the most expensive disinfectants and raised the operation cost from 27.4%-64.4% in all the scenarios tested. While UV, NaOCl, and ozone increased the cost 14.9-18.2%, 13.7-17.7% and 33.1-60.6% separately. In a UV/PAA pilot test in 2003, among all the test conditions combining PAA treatment (2 and 4 ppm) and UV irradiation (165 and 192 mJ/cm^2), the most cost-efficient condition to meet the Italian regulation was 2 ppm of PAA with 192 mJ/cm^2 UV irradiation at a cost of 0.031 Euro/m^3 (Caretti and Lubello, 2003).

5.3 Summary: advantages, concerns, and research needs

PAA is an organic peracid that displays a broad spectrum of antimicrobial activity. It is an environmental-friendly alternative to chlorine-based compounds for wastewater disinfection due to the low costs of implementation and operation and easy retrofit of the already existing equipment for chlorination (Henao et al., 2018). The associated hydrogen peroxide fraction can help to minimize the formation of DBPs and little or no PAA persists after treatment. Even so, small amounts of PAA may not have any adverse human or ecological health effects. For example, there is no evidence of any endocrine disruption potential of PAA in human health or in the ecotoxicological studies.

The physical and chemical characteristics of PAA have been widely studied, including the molecular structure, Lewis structure, bond strength and standard potential of PAA. The anti-microbial ability of PAA along with the low byproduct formation potential property made PAA a favored alternative disinfection of chlorine in water treatment. When activated by UV irradiation or catalysts, PAA generates selective reactive oxidative species including hydroxyl radicals, $CH_3C(O)OO\bullet$, and $HO_2\bullet$. The PAA based AOPs are effective to degrade poorly biodegradable contaminants and ESOCs.

In drinking water treatment, the PAA properties including PAA decay mechanisms and kinetics were studied. The PAA decay kinetics in surface water, the contribution and mechanism of PAA on the control of DBP formation from drinking water chlorination require further explorations. The objective of this research was to study the ability of PAA pre-oxidation on the control of DBP formation during subsequent chlorination in different testing scenarios, and to explore an optimum PAA pre-oxidation condition in bench scale surface water treatment.

6 Methods and Materials

6.1 Chemicals and Instruments

Peracetic Acid (PAA) used in this work was from VigorOx® WWTII, containing 15% PAA and 23% H_2O_2 (from PeroxyChem, Philadelphia, PA). Sodium hypochlorite (NaOCl) was purchased from Sigma-Aldrich; 2,2′-Azino-bis (3-ethylbenzothiazoline-6-sulfonic acid) diammonium salt (ABTS) was from Sigma-Aldrich and Pierce® horseradish peroxidase from ThermoFisher for H_2O_2 measurement. A Pocket colorimeter (HACH Chemical Co.) was used for determining total and free chlorine as well as PAA. This test is based on the DPD colorimetric method and uses pre-made DPD test kits (HACH Chemical Co.). A spectrophotometric method was used for H_2O_2 determination using a HACH DR6000 spectrophotometer. Trihalomethanes (THMs) and haloacetic acids (HAAs) were determined using conventional methods employing gas chromatography and electron capture detection (GC/ECD).

6.2 Raw Water Collection and Sample Handling.

Raw water was collected from Metacomet Lake and Windsor Pond and transported in HDPE carboys to Elab II where they were stored in 4°C in a walk-in cold room.. Raw water was filtered through 0.45micron GF/F filters before use. The filtered samples were then partitioned into clean glassware. For dark tests (i.e., no light treatment), four 300 mL volumes of filtered water were poured into separate BOD bottles and kept in 20 °C incubation in the dark. Experiments were started when

samples reached 20°C. For sunlight tests, four 500mL volumes of filtered water was poured into separate 1000mL beakers and stored outdoors under direct sunlight. The samples were kept indoor overnight and moved back to outdoor same spot the following day. The tops of the beakers were sealed with light-through plastic wraps to avoid contamination.

6.3 PAA/Peroxide Decay Test.

PAA decay kinetics were studied in bench scale. Small volumes of PAA solutions were added to the filtered water samples so that the doses were: 0, 0.5, 1.0 and 1.5 mg/L., The PAA and H_2O_2 residuals were tested every 2 hours within the first 12 hours and from there every 24 hours until 72 hours. These doses were based on mg of PAA per liter of water, and the HACH measurements corresponded to the residuals of PAA in the samples. Concentration of the stock solution was determined by HACH DPD method each time before dosing. And then a specific volume of the stock solution was diluted into each sample to reach the designed dosage. The measurements by HACH DPD method represented the amounts of total oxidants reacted with DPD, including PAA and H_2O_2. Henao et al. (2018) confirmed that no interference of H_2O_2 was expected in the measurement of low concentrations of PAA (<1.75ppm) within 60s after adding DPD. This conclusion agreed with the patent of Howarth et al. (2010) and the PAA determination method by HACH, which suggested to record the readings between 45-60s after adding DPD. Therefore, the HACH measurements represented the concentrations of PAA in samples. The decay tests were conducted under two scenarios: 20°C in the dark, and ambient outdoor temperature under direct sunlight. Weather conditions during the sunlight tests were recorded and can be found in the appendix. In the first scenario, 300 mL samples were kept in each BOD bottle in the 20°C incubation refrigerator. Residuals were tested at 0, 2, 4, 6, 8, 10, 12, 24, 48, and 72 hours. In the second scenario, 500 mL samples were kept in 1000mL beakers sealed with plastic wrap outdoors under direct sunlight. Residuals were tested at 0, 2, 4, 6, 8, 10, 24, 26, 28 and 30 hours, which included 0, 2, 4, 6, 8, 10, 12, 14, 16, and 18 hours with direct sunlight.

As stated previously, PAA concentrations were determined in accordance with the HACH total chlorine DPD method. Hydrogen peroxide (H_2O_2) concentration was measured using the ABTS (Diammonium 2,2′-azino-bis(3-ethylbenzothiazoline-6-sulfonate)) UV absorbance method with determination at a wavelength of 415 nm. The test procedures are attached in the appendix.

6.4 Chlorination

The samples with same test conditions were chlorinated at the same chlorine dose (either 2.3 or 7.74 mg/L) after the PAA pre-oxidation for three days, during which the samples were stored in 1-liter glass bottles in a 20°C incubator. Then the 1-liter samples were separated into 3 BOD bottles for subsequent reaction at chlorine contact times of 6, 24 and 72 hours. Chlorine was dosed at 2.3 mg/L and 7.74 mg/L as Cl_2 separately for raw water from Metacomet Lake (Springfield, MA) and Windsor Pond (MA), respectively.

Chlorine doses were determined by preliminary demand testing of raw water and pre-oxidized water. The 6-hour chlorine demand of PAA pre-oxidized raw water was determined by adding different doses of chlorine to the raw water and measuring the residual after 6 hours. The chlorine demand was the amount of chlorine lost during those 6 hours when leaving a residual of 2 mg/L.

6.5 Disinfection Byproduct Formation Potential Test

THMs were determined by liquid/liquid extraction with pentane followed by GC/ECD according to USEPA method 551.1. HAAs were analyzed by liquid/liquid extraction with methyl-tertiary-butyl-ether (MtBE) followed by derivatization with acidic methanol and quantified by GC/ECD according to USEPA method 552.2. (Jiang et al, 2019)

7 Result and Discussion

7.1 PAA Pre-disinfection Under 20 C in Dark

7.1.1 Peracetic Acid and Hydrogen Peroxide Decay Under 20 C° in Dark

The PAA decay kinetics in raw water was studied. The tests were conducted on the raw water from Metacomet Lake with a SUVA value of 3.06 L/ (mg m) and pH 6.2. The decay test lasted 72 hours at which time the PAA residual in all samples had dropped below 0.5 mg/L. Results for both PAA and hydrogen peroxide are shown in Figure 6. Given the three mass-based PAA doses (0.5, 1.0 and 1.5 ppm), the expected molar compound doses were: 0.0066, 0.0132 and 0.0197 mM for PAA and 0.0226, 0.0451 and 0.0677 mM for H_2O_2, respectively. The initial H_2O_2 measurements, which were 0.0503, 0.1045 and 0.1520 mM, were about 127% higher than expected based on the PAA dose and the ratio of H_2O_2 to PAA as indicated by the manufacturer. This may be due to incorrect information from the manufacturer on the product's H_2O_2/PAA ratio, or to some unknown positive bias in the analysis of residual hydrogen peroxide.

Both PAA and hydrogen peroxide were examined (rate constants in table 2) for their agreement with first order decay (Figure 7.1 – 7.4) and second order decay (Figure 8.1 – 8.6). The decay of high PAA doses (1.0 ppm and 1.5 ppm) was observed as first order in PAA throughout the whole reaction

time with rate constants of 0.0006 and 0.0003 min^{-1} and R^2 values of 0.9972 and 0.9967 separately. The decay of the low PAA doses (0.5 ppm) was modeled more accurately as two first-order reactions with a break point at 600 min. The rate constants for the two processes were 0.0015 and 0.0007 min^{-1} and R^2 values were 0.9975 and 0.9119 separately. The result of the low PAA dose (0.5 ppm) decay test corroborated with the study of da Silva et al. (2020) which also observed a rate constant drop after 150 min.

Hydrogen peroxide decay kinetics were studied since this is in equilibrium with PAA and acetic acid. Hydrogen peroxide (H_2O_2) decay was slower than PAA decay when both were modeled as first-order reactions. The hydrogen peroxide decay processes in all three cases in this study could be divided into two parts. The break point of low PAA dose (0.5 ppm) was 480 min and the break point of high PAA doses (1.0 ppm and 1.5 ppm) was 720 min. The rate constants for the first half of the H_2O_2 decay were 0.0003, 0.0001 and 0.00007 min^{-1} with R^2 values of 0.9211, 0.9208 and 0.9651 for 0.5, 1.0 and 1.5 ppm separately, and the rate constants for the second half of the H_2O_2 decay were 0.00008, 0.00006 and 0.00005 min^{-1} with R^2 values of 0.9226, 0.9286 and 0.9417. The decay rate of low PAA doses were higher than those of high PAA doses. The decay rate dropped with contact time as less H_2O_2 remained in the solution. After the 72-hour decay process, H_2O_2 became the domain species in the sample.

The decay of PAA and H_2O_2 were modeled as seconded-order reactions to compare with the first-order models. When modeling throughout the whole reaction times, the decay rate constants of PAA were 1.1822, 0.2741 and 0.0428 with R^2 values of 0.9773, 0.8629 and 0.9531 in the scenarios where PAA doses were 0.5, 1.0 and 1.5 ppm separately. The decay rate constants of H_2O_2 were 0.0027, 0.0009 and 0.0004 with R^2 values of 0.9379, 0.9574 and 0.9728 in the scenarios where PAA doses were 0.5, 1.0 and 1.5 ppm separately. When dividing the decay into two parts with a break point at 720 min, the decay rate constants of PAA decay in the first parts of the reactions were 0.3768, 0.0638 and 0.0251 with R^2 values of 0.9801, 0.9906 and 0.9918 in the scenarios where PAA doses were 0.5, 1.0 and 1.5 ppm separately. The decay rate constants of H_2O_2 decay in the first parts of the reactions were 0.0052, 0.0014 and 0.0004 with R^2 values of 0.9388, 0.9288 and 0.9636 in the scenarios where PAA doses were 0.5, 1.0 and 1.5 ppm separately. The R^2 values of 0-720min in the two-parts models are higher than the R^2 values of the whole reaction time models, implying that the H_2O_2 decay could be modeled more accurately as two second-order reactions with a break point at 720 min.

Comparing the R^2 values of different models (Table 2), PAA decay was more accurately modeled as first-order reactions since the R^2 values of the first-order modeling were higher than those of the second-order modeling. The decay of PAA with 0.5 ppm PAA dose was modeled as two first-order reactions with a breakpoint at 480 min. The decay of PAA with 1.0 and 1.5 ppm PAA doses was modeled as a first-order reaction throughout the whole reaction time. The decay of H_2O_2 aligned more

accurately with second-order models. The decay of H_2O_2 with 0.5 ppm PAA dose was modeled as two second-order reactions with a breakpoint at 480min. The decay of H_2O_2 with 1.0 and 1.5 ppm PAA doses was modeled as a second-order reaction throughout the whole reaction time.

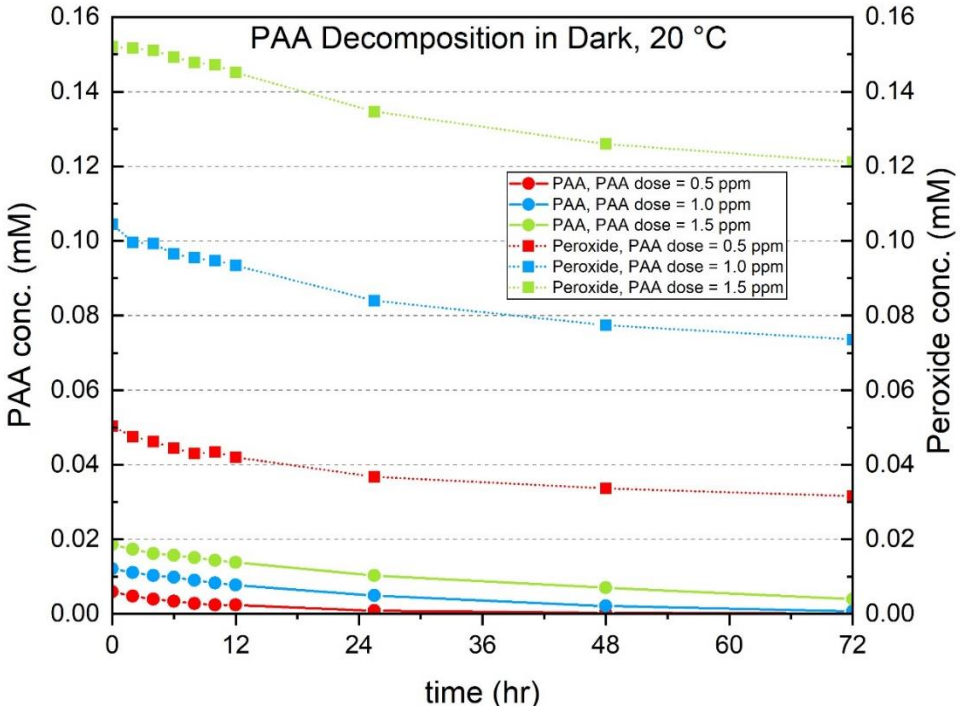

Figure 6. PAA and Peroxide Decomposition in Lake Metacomet Water (Dark, 20°C)

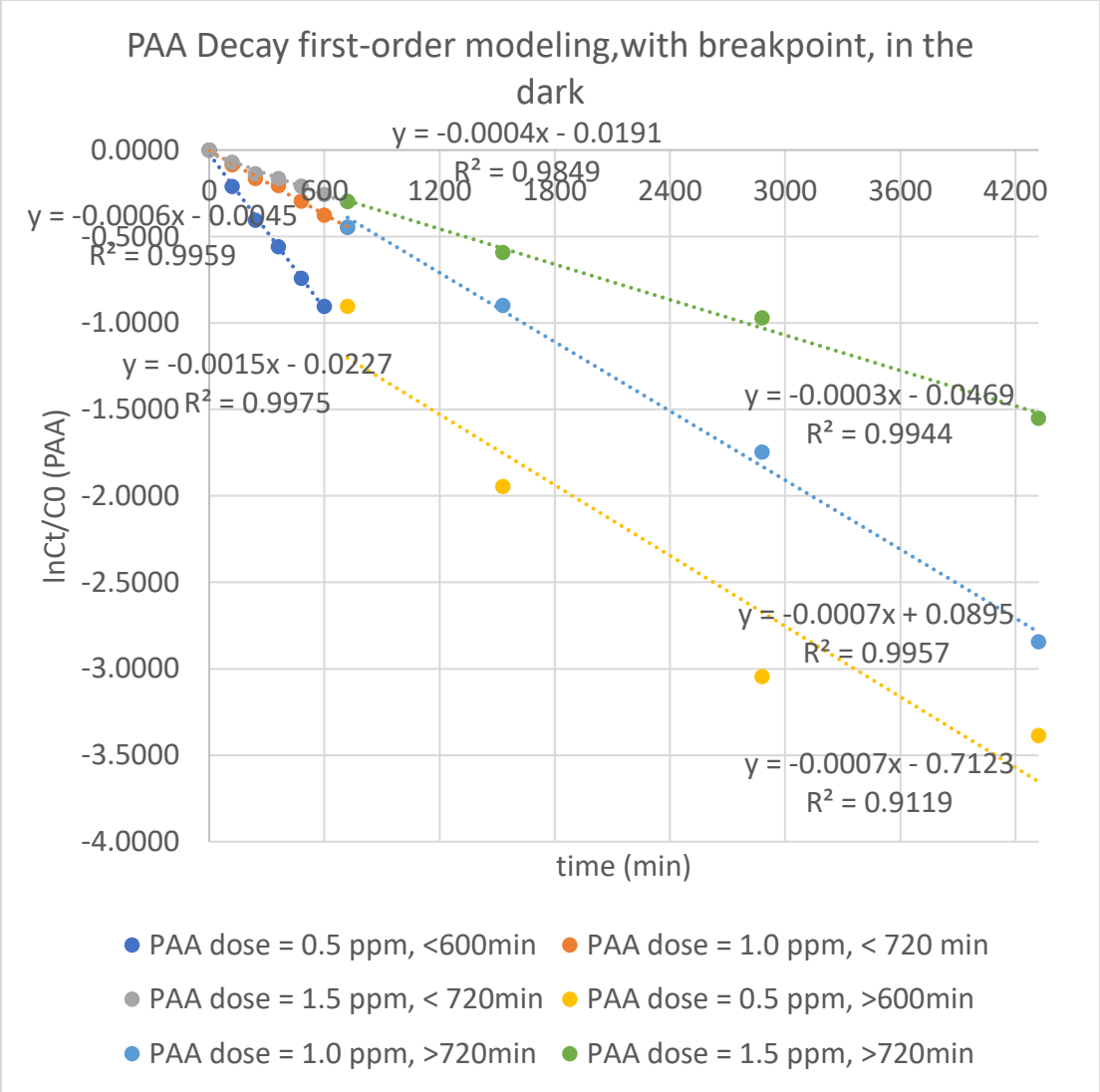

Figure 7.1. PAA Decay first-order modeling, with breakpoint, in the dark

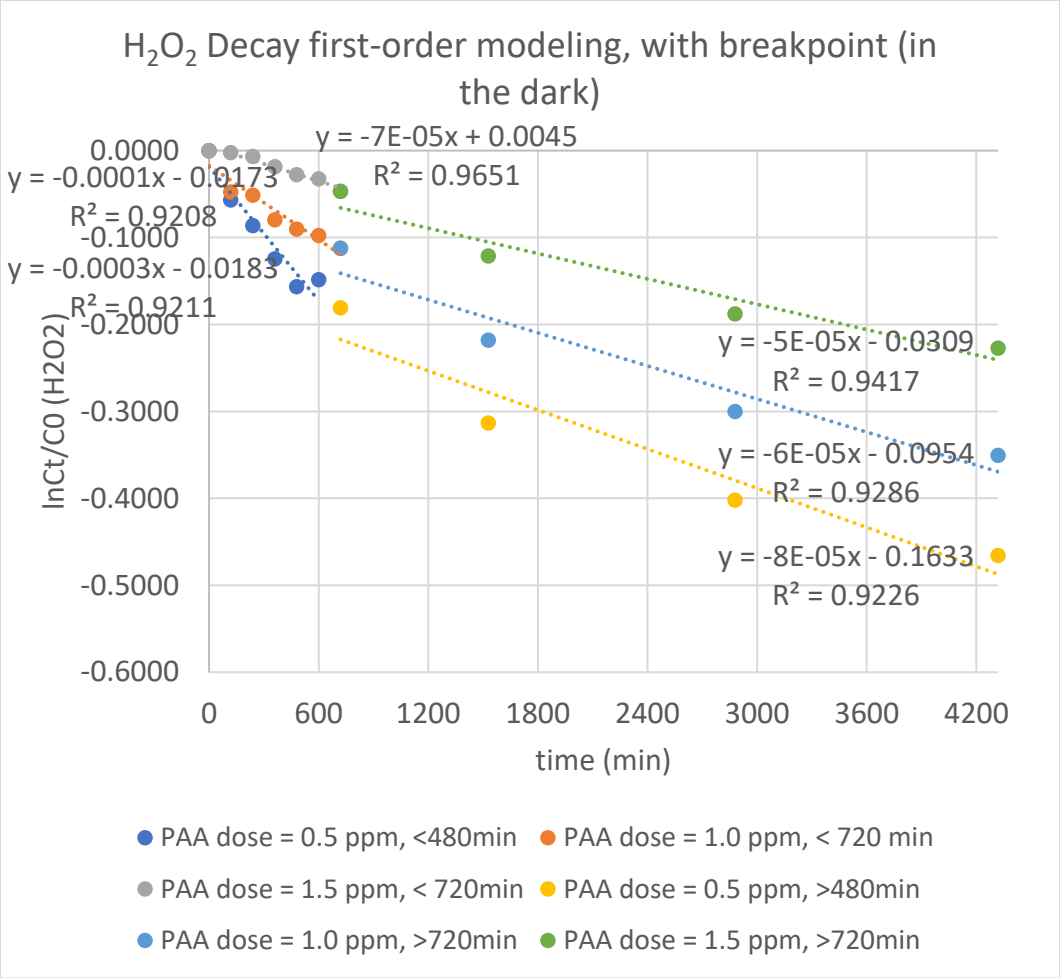

Figure 7.2. H_2O_2 Decay first-order modeling, with breakpoint (in the dark)

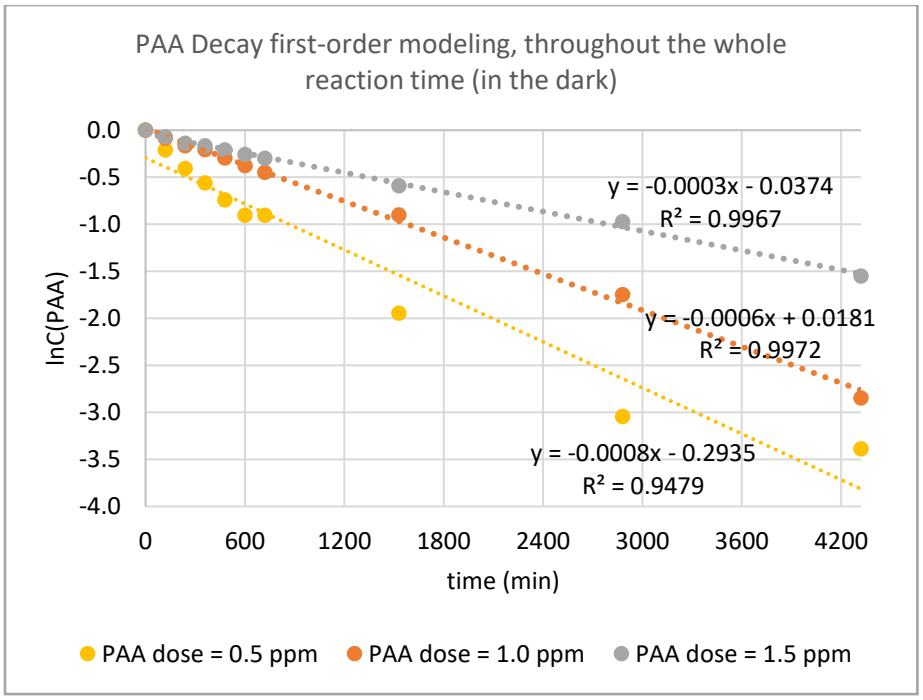

Figure 7.3. PAA Decay first-order modeling, throughout the whole reaction time (in the dark)

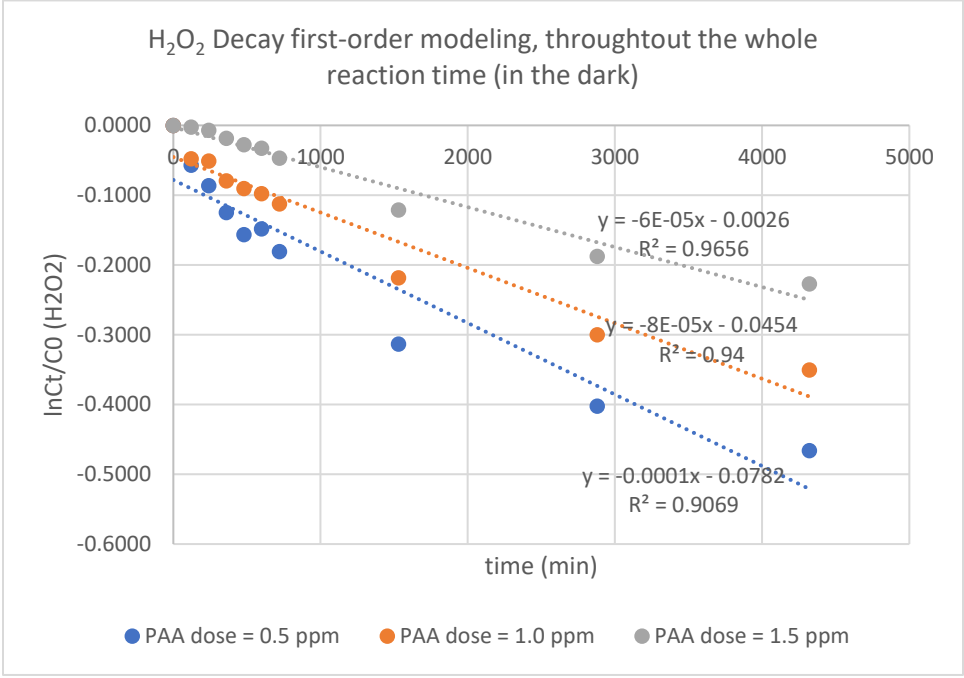

Figure 7.4. H_2O_2 Decay first-order modeling, throughout the whole reaction time (in the dark)

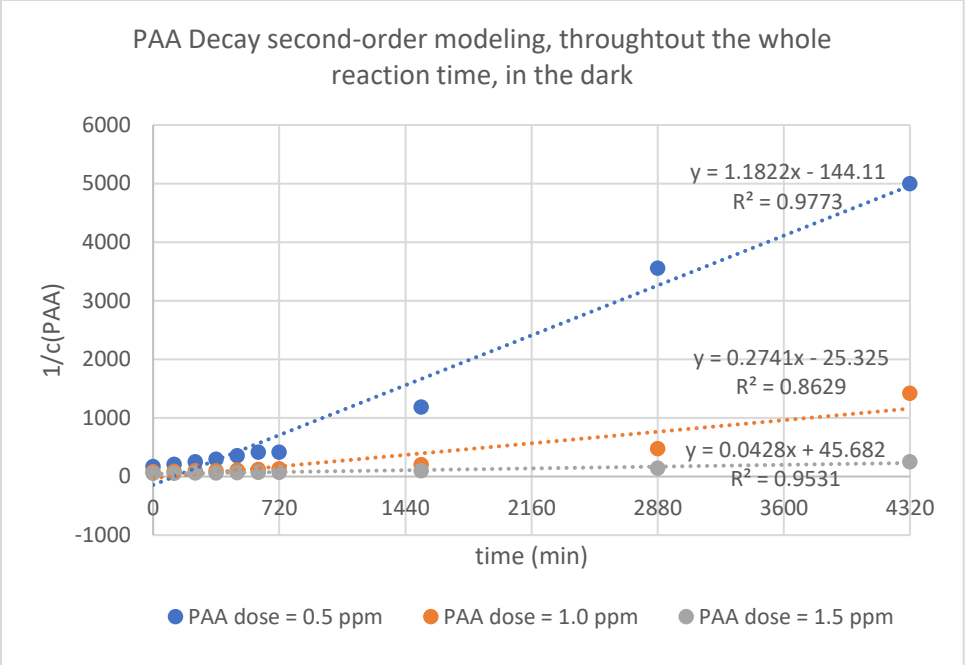

Figure 8.1 PAA Decay second-order modeling, throughout the whole reaction time, in the dark

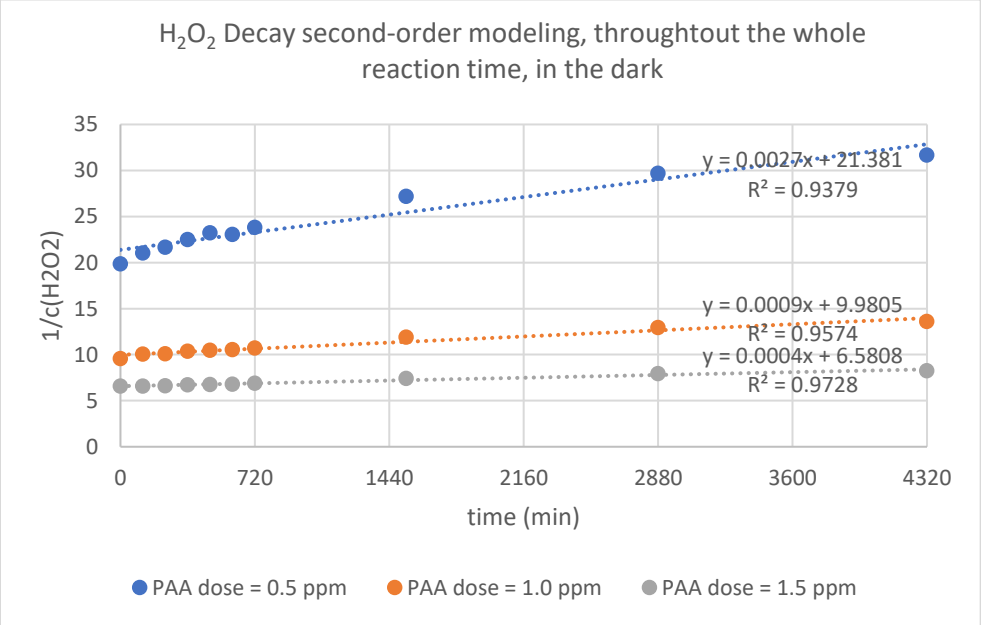

Figure 8.2 H2O2 Decay second-order modeling, throughout the whole reaction time, in the dark

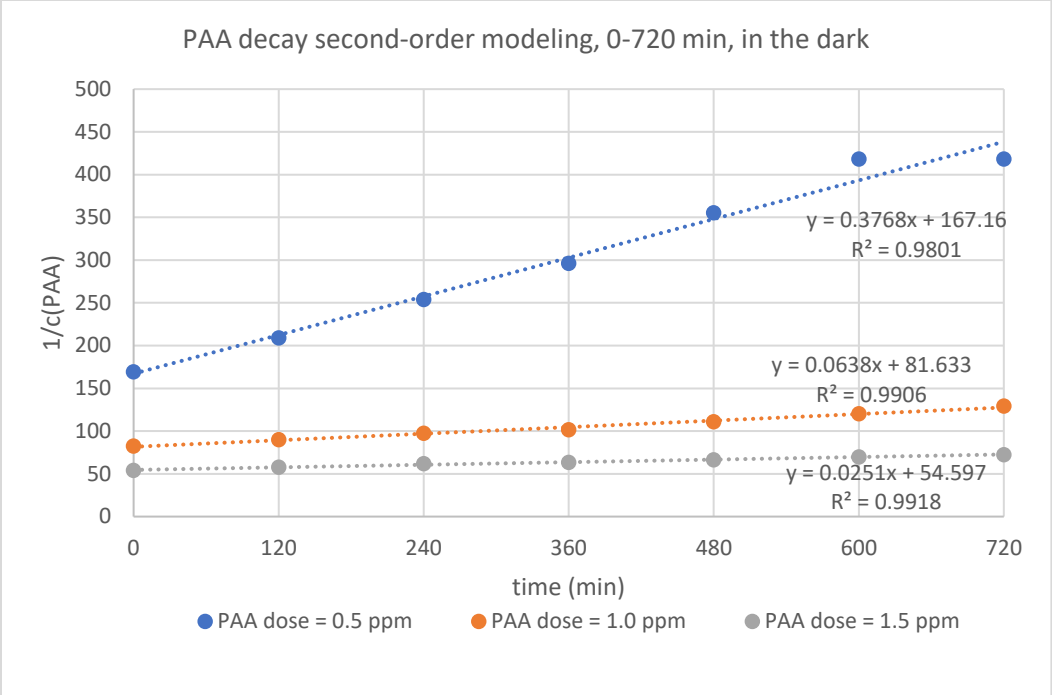

Figure 8.3 PAA decay second-order modeling, 0-720 min, in the dark

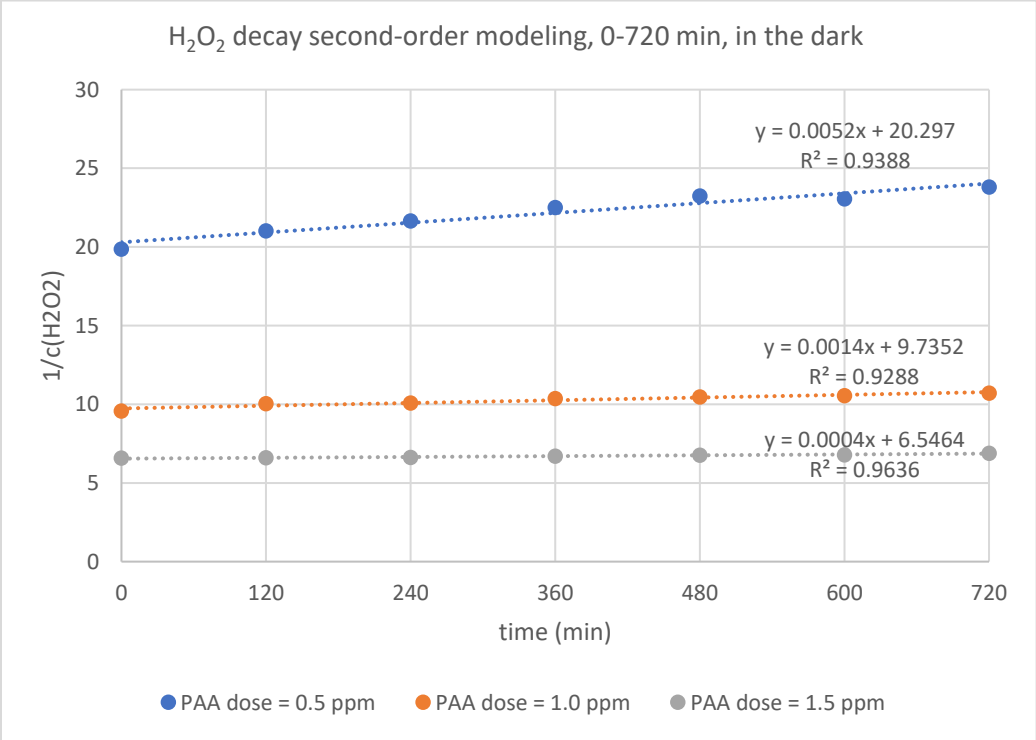

Figure 8.4 H_2O_2 decay second-order modeling, 0-720 min, in the dark

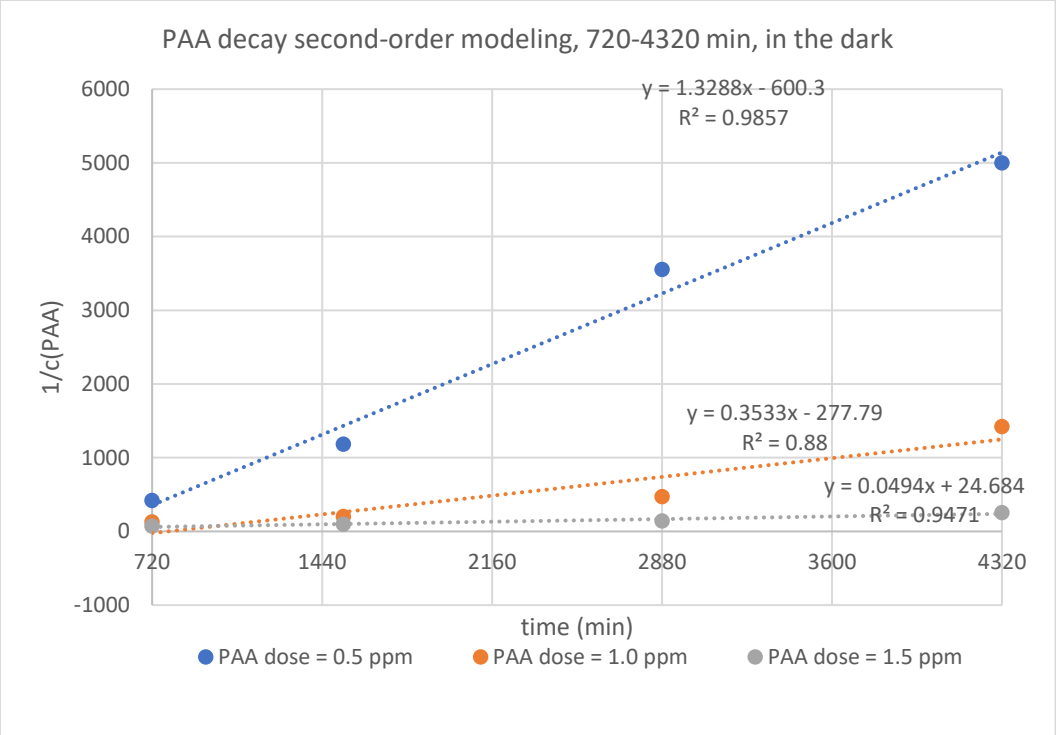

Figure 8.5 PAA decay second-order modeling, 720-4320 min, in the dark

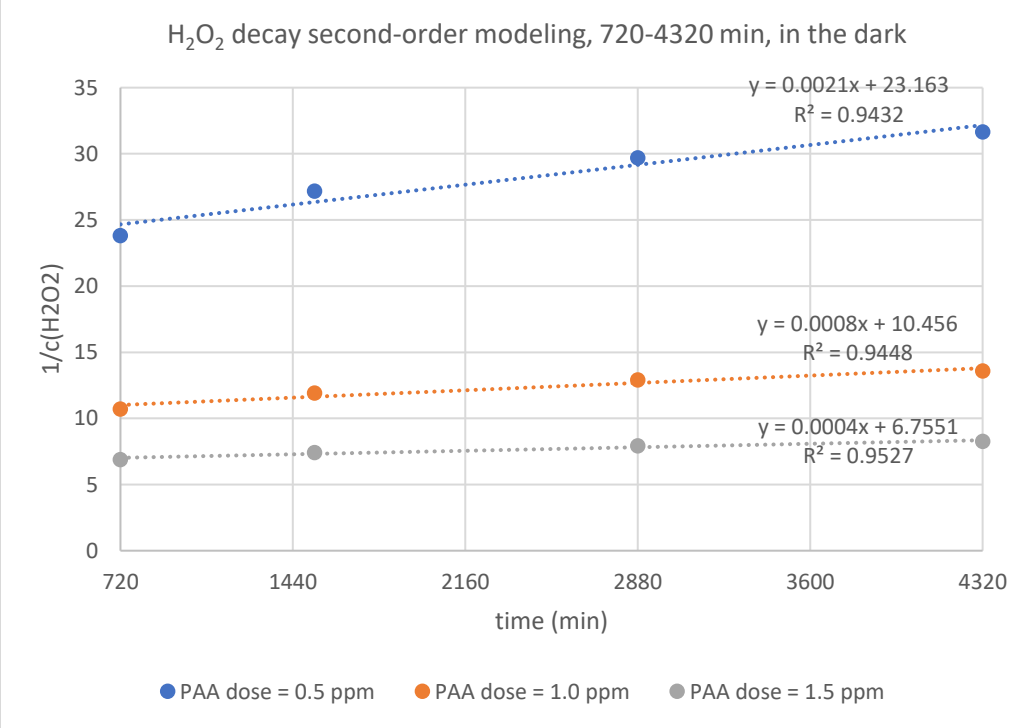

Figure 8.6 H_2O_2 decay second-order modeling, 720-4320 min, in the dark

Table 2.1 Rate constants and R^2 values of the First-order Modeling of PAA and H_2O_2 Decay

1st-order kinetics modeling		throughout the whole reaction time		two parts, breakpoint: 480 min for 0.5 ppm dose; 720min for 1.0, 1.5 ppm dose			
				first part		second part	
component	PAA dose (ppm)	rate constant (min^{-1})	R^2	rate constant (min^{-1})	R^2	rate constant (min^{-1})	R^2
PAA	0.5ppm	0.0008	0.9479	0.0015	0.9975	0.0007	0.9119
	1.0ppm	0.0006	0.9972	0.0006	0.9959	0.0007	0.9957
	1.5ppm	0.0003	0.9967	0.0004	0.9849	0.0003	0.9944
H_2O_2	0.5ppm	0.0001	0.9069	0.0003	0.9211	0.00008	0.9226
	1.0ppm	0.00008	0.9400	0.0001	0.9208	0.00006	0.9286
	1.5ppm	0.00006	0.9656	0.00007	0.9651	0.00005	0.9417

Table 2.2 Rate constants and R^2 values of the Second-order Modeling of PAA and H_2O_2 Decay

2nd-order kinetics modeling		throughout the whole reaction time		two parts, breakpoint: 720min			
				first part		second part	
component	PAA dose (ppm)	rate constant ($mM^{-1}\ min^{-1}$)	R^2	rate constant ($mM^{-1}\ min^{-1}$)	R^2	rate constant ($mM^{-1}\ min^{-1}$)	R^2
PAA	0.5ppm	1.1822	0.9773	0.3768	0.9801	1.3288	0.9857
	1.0ppm	0.2741	0.8629	0.0638	0.9906	0.3533	0.8800
	1.5ppm	0.0428	0.9531	0.0251	0.9918	0.0494	0.9471
H_2O_2	0.5ppm	0.0027	0.9379	0.0052	0.9388	0.0021	0.9432
	1.0ppm	0.0009	0.9574	0.0014	0.9288	0.0008	0.9448
	1.5ppm	0.0004	0.9728	0.0004	0.9636	0.0004	0.9527

7.1.2 Chlorine Demand

Figure 9 shows that chlorine demand is related to the PAA dose and chlorine contact time. Except for the highest dose, the chlorine demand of the PAA pre-oxidized water was lower at contact times of 6 and 24 hours than that of raw water alone. It is likely to be the result of destruction of chlorine-

reactive sites in natural organic matter by PAA. With higher PAA doses, less chlorine-demanding sites in natural organic matter are left. However, the chlorine demand appeared higher with the highest PAA dose (1.5 mg/L). The DBP formation potential data implied that instead of producing more reactive sites in NOM, the chlorine demand was actually caused by the high H_2O_2 residual. The chlorine residual dropped to 0 within 6 hours with 1.5 mg/L PAA pre-oxidation, because all chlorine was consumed by the hydrogen peroxide residual from PAA decomposition.

Chlorine demand can be considered as the sum of two parts: the demand of the H_2O_2 residual and that of NOM. The NOM-based chlorine demand can be calculated by subtracting the estimated H_2O_2-based chlorine demand from the total observed chlorine demand. The H_2O_2-based chlorine demand can be calculated using the measured hydrogen peroxide residual and the known chlorine- H_2O_2 stoichiometry. The results for this calculation are shown in figures 10.1 to 10.3 below. These indicate a negative chlorine demand for NOM after reaction with PAA, which is clearly not possible. Once again this points to a possible positive bias in the hydrogen peroxide measurements.

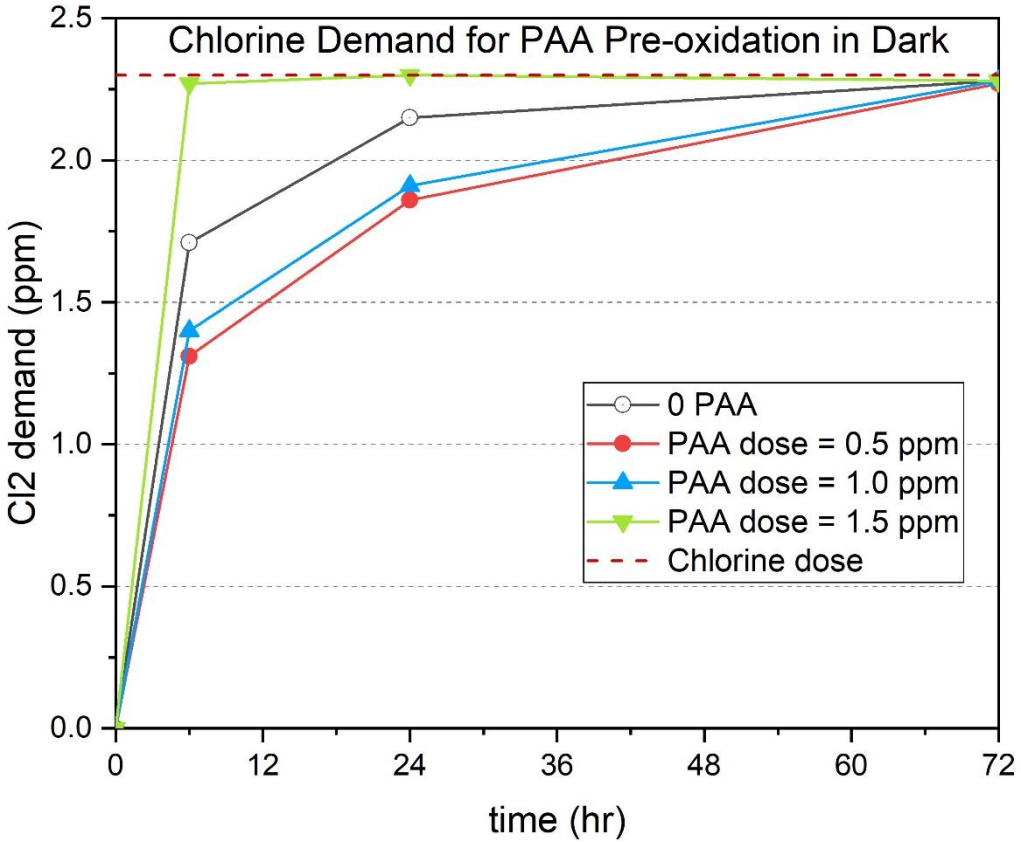

Figure 9. Chlorine Demand for PAA Pre-oxidation as a Function of Chlorine Contact Time (in the Dark, 20 C°)

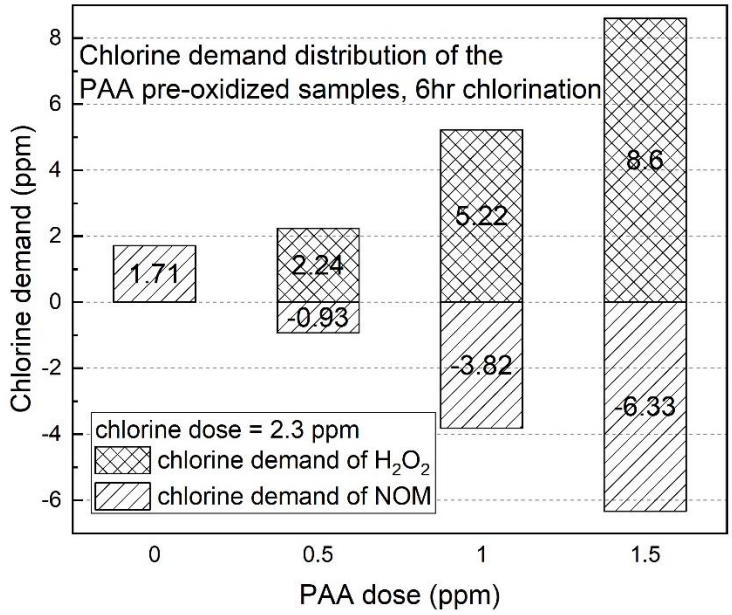

Figure 10.1 Theoretical chlorine demand distribution of PAA pre-oxidized samples, 6-hour chlorination (in the dark)

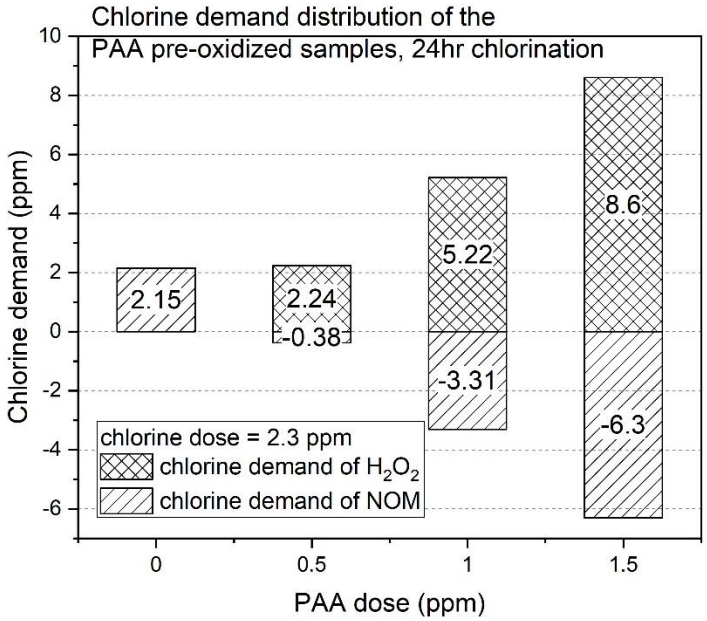

Figure 10.2 Theoretical chlorine demand distribution of PAA pre-oxidized samples, 24-hour chlorination (in the dark)

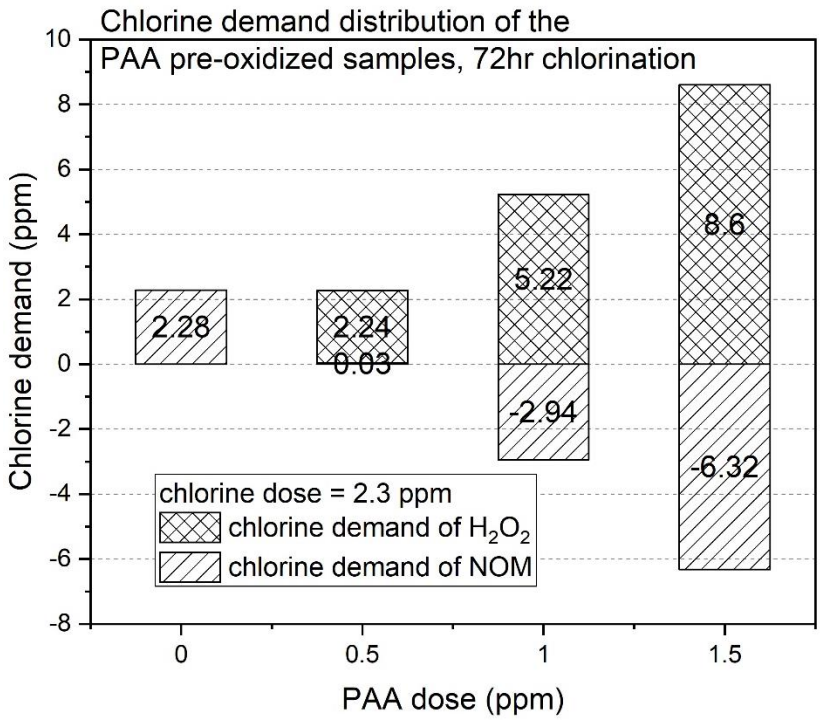

Figure 10.3 Theoretical chlorine demand distribution of PAA pre-oxidized samples, 72-hour chlorination (in the dark)

7.1.3 Control Effect of PAA Pre-oxidation in Dark on THMs and HAAs Formation Potential

Even though there were obvious anomalies in the estimated chlorine demand of NOM for PAA pre-disinfected samples, the DBPFP results seemed to reflect the total chlorine demand. Figure 11 shows that pre-oxidation with PAA depressed the THM and HAA formation potential for all chlorine contact times tested. The impact of PAA was greater with higher doses of PAA. Comparing to raw water chlorination, with 0.5 mg/L PAA pre-oxidation, the THM4 formation potential is 21% lower than that of raw water without PAA and HAA5 formation potential is 25% lower than that of raw water with chlorine alone after 6-hour chlorination. THM4 and HAA5 formation potential were 8% and 14% lower than those of raw water without PAA separately after 24-hour chlorination. THM4 and HAA5 formation potential were 6% and 12% lower than those of raw water with chlorine alone separately after 72-hour chlorination. 1.0 mg/L PAA has better control effect. 33% and 32% decrease of THMs and HAAs formation potential was observed after 6 hours chlorine contact time. 23% and 22% decrease of THMs and HAAs formation potential was observed after 24 hours chlorine contact time. 13% and 34% decrease of THMs and HAAs formation potential was observed after 72 hours of chlorine contact time. It should be noted that other electrophilic pre-oxidants such as ozone and

chlorine dioxide have also been observed to result in THM and HAA precursor destructions in the range of 6-34%. Finally, a 1.5mg/L PAA dose appeared to destroy more than 90% of THM and HAA precursors. According to the explanation in part 7.1.2, high concentrations of H_2O_2 residual likely consumed the chlorine before it had much of a chance to reaction with NOM. Thus the low DBP formation potential was not controlled by PAA but rather it was the lack of a chlorine residual.

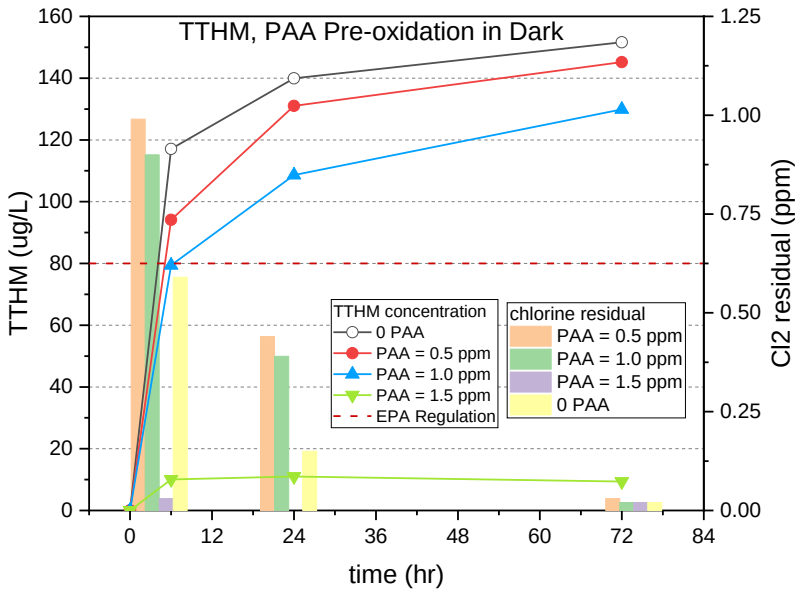

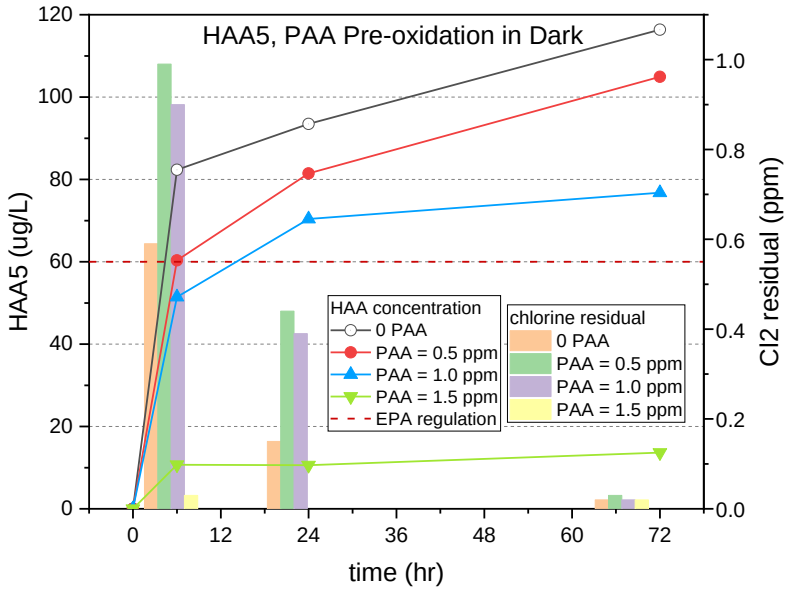

Figure11. TTHM and HAA5 Level vs Chlorine Contact Time with PAA -Pre-oxidation in Dark, 20 C°

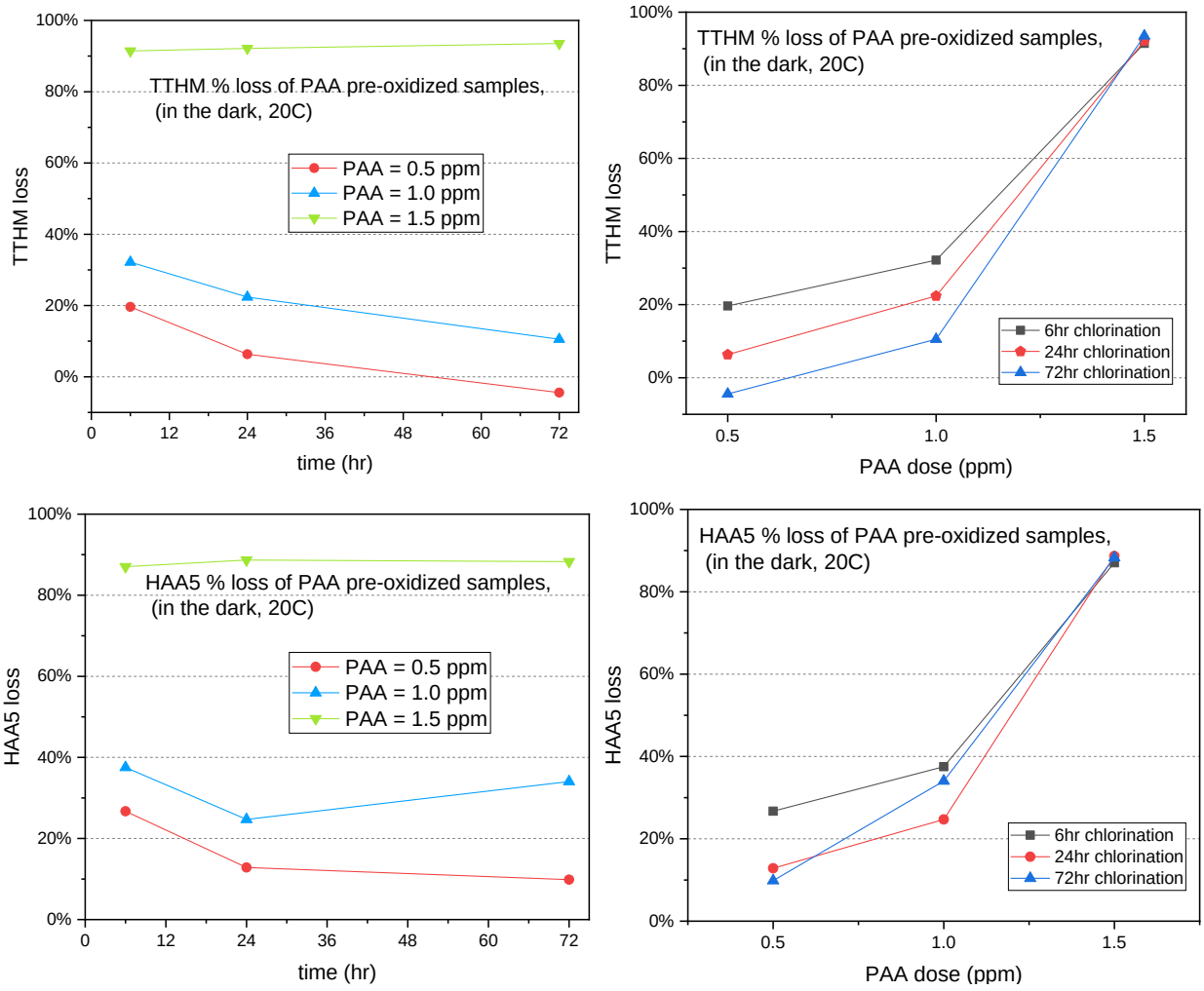

Figure 12. TTHM and HAA5 % decrease of PAA pre-oxidized samples (in the dark, 20C)

7.2 PAA Pre-disinfection Under Direct Sunlight

7.2.1 PAA and Peroxide Decay Under Direct Sunlight

The PAA decay behavior in the filtered Windsor Pond water under direct sunlight was also studied. Sunlight accelerated the process as PAA residual in each sample was below 0.5mg/L after 18 hours of direct sunlight exposure. This was much faster than the 72-hour decay process when conducted in the dark. The peroxide residuals were similar to those at the end of the dark PAA decay. However, the peroxide decay rate constants were higher in sunlight than those determined for PAA in the dark. The decay curve alone is not able to show whether sunlight accelerated the PAA decay

process or it accelerated the reaction of PAA with NOMs, or both. Chlorination and DBPFP tests were conducted for further understanding of the whole process.

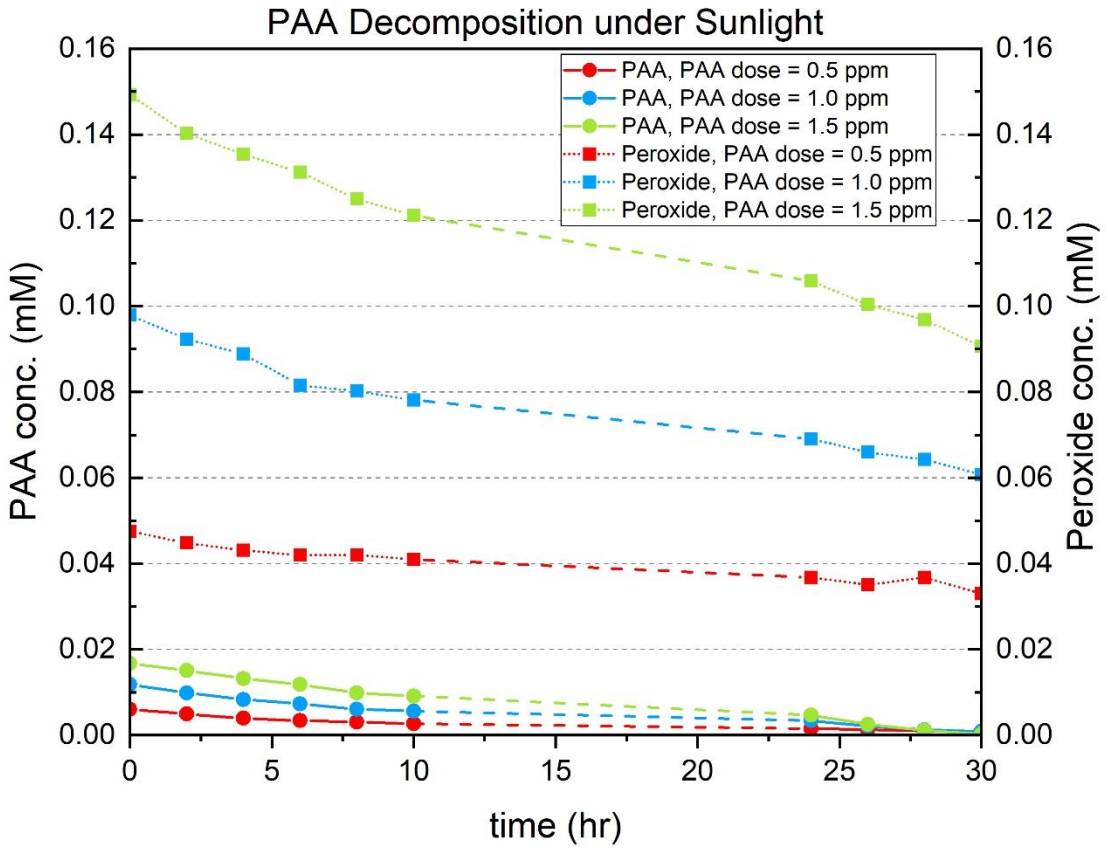

Figure 13. PAA and Peroxide Decomposition in Windsor Pond water, (under Sunlight)

7.2.2 The Effect of PAA Pre-disinfection Under Direct Sunlight on DBP Control

The DBPFP results (figure15, 16) showed that PAA had indeed destroyed precursors under sunlight. The THM and HAA levels in the sample treated with 0.5 mg/L of PAA were close to the sample without PAA pre-oxidation. However, in the sample with 1.0 mg/L PAA dose, there was 22.6% decrease of THMs and 34% decrease of HAAs compare to the sample without PAA pre-treatment. The sample dosed with 1.5 mg/L PAA showed even more loss of DBP formation. THMs and HAAs were 63.9% and 82.1% less than the sample without PAA treatment.

The two parts of chlorine demand, by NOM and peroxide residual, were calculated in table 3. Again, the chlorine consumption by H_2O_2 is assumed to occur according to a molar stoichiometry of 1:1. The chlorine demand by hydrogen peroxide was then converted into mg/L. As before, the chlorine demand of NOM was the difference between the total demand and the demand by hydrogen peroxide. Figure 14 shows the chlorine demand attributed to NOM and to hydrogen peroxide. The NOM-based

chlorine demand decreased when the dose of PAA increased, suggesting that higher doses of PAA consumed more chlorine-reactive sites on NOM. The DBPFP of the sample with 0.5 ppm PAA dose generated slightly more TTHM and HAA5 than the control sample. The DBPFPs of samples with 1.0 ppm and 1.5 ppm PAA dose showed similar trends with chlorine demand where samples treated with higher PAA doses generated less TTHM and HAA5. The THMFP of the 1.0 ppm dose samples in the dark test and sunlight test were 13% and 22.6% lower than the control samples, respectively. The HAAFPs of the 1.0 ppm dosed samples in the dark test and sunlight test were both 34% lower than the control samples. The THMFP results implied that sunlight not only accelerated the PAA decomposition but also enhanced the PAA oxidation of NOM. This agreed with the study by J. Hollman et al. (2020) that UV could activate PAA to form various reactive radicals. However, considering the low chlorine residual (figure 16), 1.04, 0.76 and 0.03 ppm in the samples with 0.5, 1.0 and 1.5ppm dose as PAA, there's possibility that the low THM and HAA formation was due to lack of chlorine. The high level of THM and HAA decrease may not be totally contributed by the pre-oxidation of PAA.

Table 3 Chlorine Demand Distribution Calculation, PAA Pre-oxidized under Sunlight

PAA dose(ppm)	0.5	1	1.5
H_2O_2 residual (mM)	0.03	0.06	0.09
Cl_2 demand of H_2O_2 (mM)	0.03	0.06	0.09
Cl_2 demand of H_2O_2 (ppm)	2.34	4.31	6.43
Total Cl_2 demand (ppm)	5.86	6.14	6.87
Cl_2 demand of NOM (ppm)	3.52	1.83	0.44

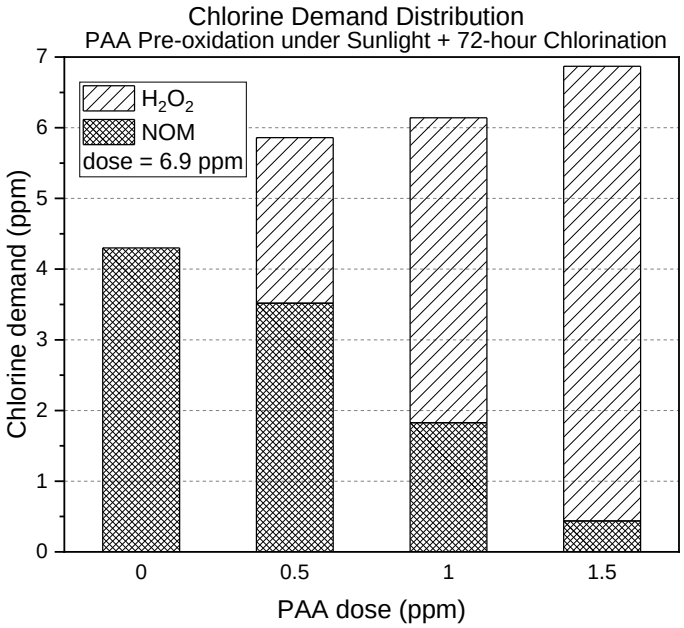

Figure 14 Chlorine Demand Distribution with PAA Pre-oxidation under Sunlight and 72-hour Chlorination

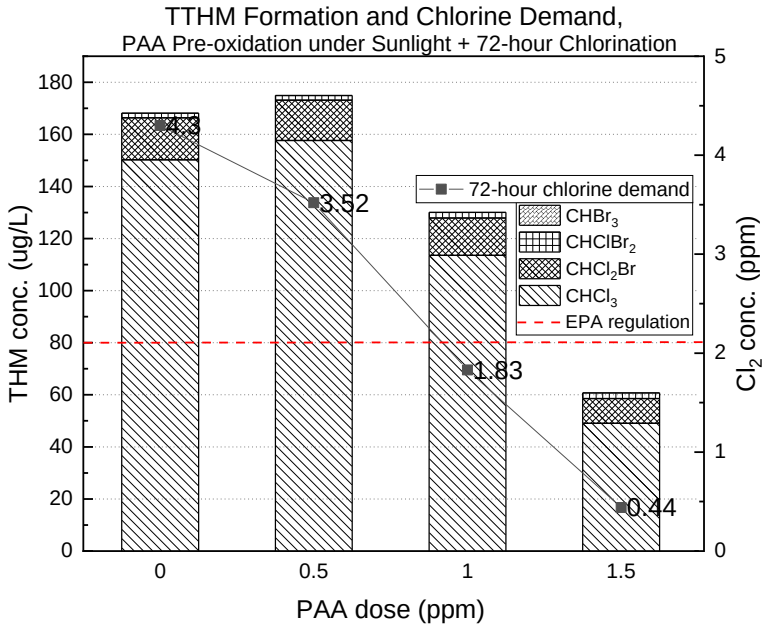

Figure 15.1 TTHM Formation and Chlorine Demand vs PAA dose with PAA Pre-oxidation under Sunlight and 72-hour Chlorination

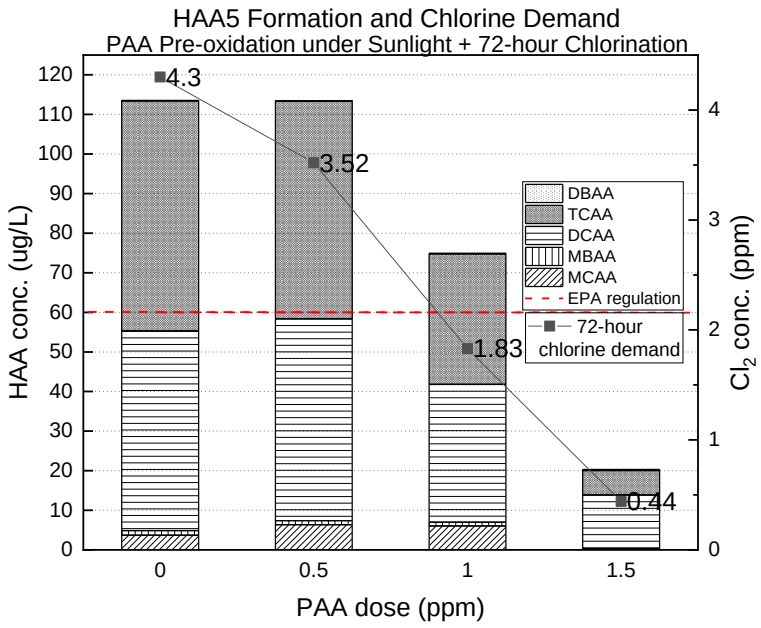

Figure 15.2 HAA5 Formation and Chlorine Demand vs PAA dose with PAA Pre-oxidation under Sunlight and 72-hour Chlorination

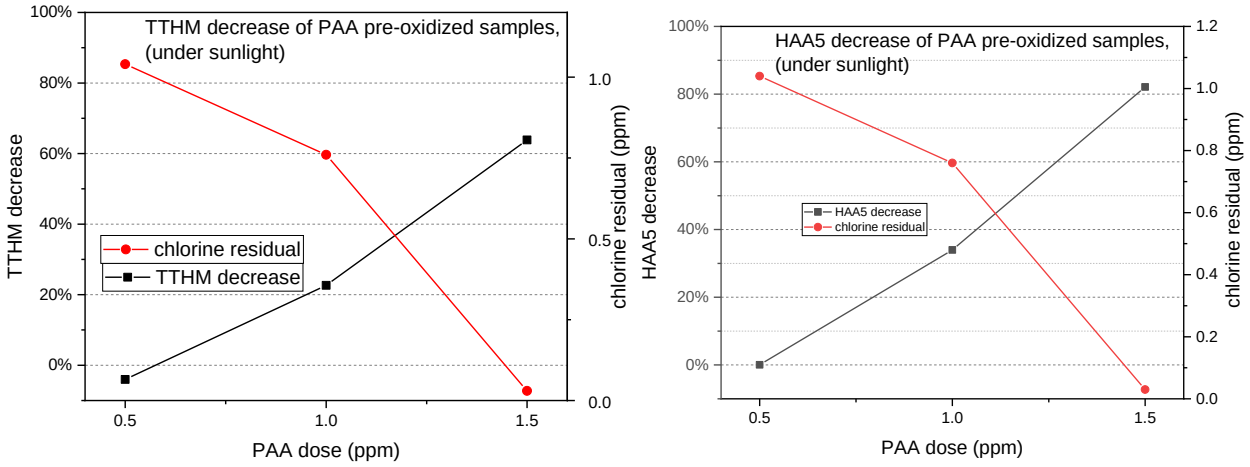

Figure 16. TTHM and HAA5 % decrease of PAA pre-oxidized samples (under sunlight)

7.3 Short PAA Contact Time Effect on PAA Pre-disinfection and DBP Control

Even though PAA showed significant destruction of DBPFP from chlorination in the previous tests, it is not usually practical or even possible in municipal water treatment plants to provide pre-

oxidation contact times of 72 hours. Thus, in the interest of application to practice, PAA pre-oxidation was studied with short contact times in the range of seconds to 24 hours.

The experiment was conducted at bench scale with four experimental variables, each variable had two to four values: PAA dose (0 and 1 ppm), PAA contact time (instant, 2, 6, 24 hr), chlorine dose (0, 7.74 ppm) and chlorine contact time (instant, 6 hr). The combinations of the four parameters simulated and compared the scenarios of:

1. Impact of PAA pre-oxidation on DBP formation from subsequent chlorination. (PAA dose as the variable)
2. Impact of PAA contact time on chlorine demand and DBP precursor destruction. (PAA contact time as the variable)
3. Impact of chlorine dose on DBPFP destruction due to PAA treatment. (chlorine dose as the variable)
4. Impact of chlorine contact time on DBPFP (chlorine contact time as the variable)

Chlorine demand, THM and HAA formation potential were tested after chlorination. The 1.0 ppm PAA dose was chosen based on the results of previous tests. It was the lowest dose among the doses tested that effectively destroyed DBP precursors while not leading to excessive loss of chlorine due to residual hydrogen peroxide. PAA and hydrogen peroxide residuals were not quenched before chlorination and the residuals were tested after PAA pre-oxidation. A 6-hour chlorine demand test was conducted before the contact time tests. The two component parts of chlorine demand were tested. The organic (i.e., NOM) chlorine demand of raw water after 6-hour chlorination was 2.14 ppm. The other chlorine demand component was determined to be 3.6 ppm, and this is interpreted as the demand of the PAA and hydrogen peroxide residual after immediately after (instant) contact with raw water. The chlorine demand of the instant PAA contact was the highest demand among all PAA contact times since the PAA and hydrogen peroxide residuals would decrease with contact time. Chlorine dose was determined to be 7.74 ppm by taking the sum of the two demands and adding the 2 ppm target residual of 6 hours chlorination with PAA pre-oxidation.

7.3.1 DBP Formation Potential by PAA Pre-oxidation

In figure 17, the HAA5 and THM4 formation with 1 ppm PAA was compared with the raw water DBP formation potential. No measureable THM4 and very little HAA5 could be found after 0-24 hours of PAA oxidation. This is not surprising as these samples had not been treated with active chlorine.

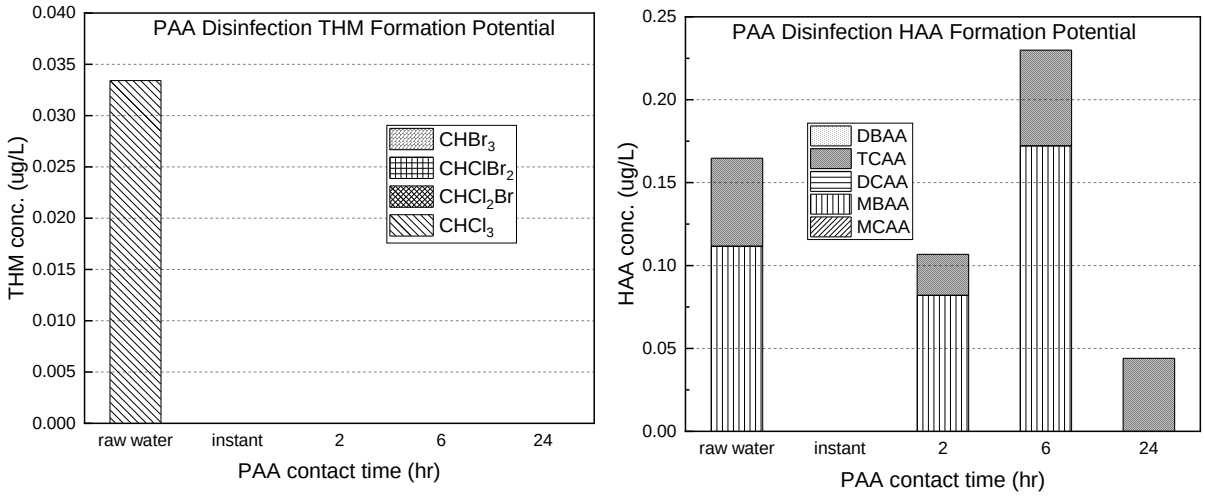

Figure 17 . PAA Disinfection THM and HAA Formation Potential

7.3.2 PAA Contact Time Effect on DBP Control

Figure 18 displayed the chlorine demands at different PAA contact times. Note that the total demand of PAA residual and NOM were considered. Chlorine demand decreased as PAA contact time increased, and the chlorine demand dropped significantly within the first 2 hours followed by a smooth decrease until 24-hr PAA contact. This implies that PAA consumes more reactive sites in NOM with longer PAA contact times, and thus resulting in lower chlorine demands. The PAA decomposition kinetics were fast in the first 2 hours and the decay rate decreased as the PAA was consumed by NOM. This observation agreed with the study of Chen and Pavlostathis (2019) and Pedersen et al. (2009), where the decomposition rate increased with higher PAA doses in the treated effluent. Chlorine demand was higher with longer chlorine contact times because chlorine's reactions with NOM are slow and continue for hours. This also implies that 1 mg/L PAA dose with up to 24 hours contact time was not able to oxidize all chlorine-reactive sites in NOM which assures some leve of subsequent reaction of chlorine with NOM and the formation of chlorinated DBPs. A final chlorine residual of 1.5-3.2 mg/L was observed throughout the test.

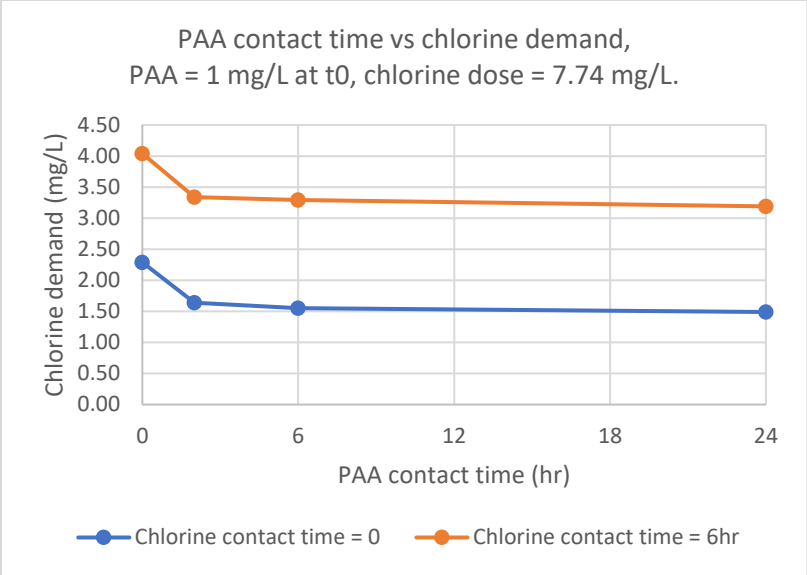

Figure 18 . Chlorine Demand vs PAA Contact Time

Figure 19 displays the concentration of DBPs formed with different PAA contact times. Less DBPs were formed during chlorination with PAA pre-oxidation than chlorination alone. The test with minimum (instant) chlorine contact showed that THMs and HAAs were able to form with very short chlorine contact times. More THMs and HAAs were formed with longer chlorine contact time.

Figure 19.2 displayed the DBPs formed after 6 hours of chlorination. HAA formation decreased as the PAA contact time increased. The lowest HAA formation potential was observed for 24 hours of PAA contact time. This value was 47.7 ug/L, representing 25.8% less than the HAA formation potential of the sample without PAA treatment. After 2 hours of PAA contact and subsequent chlorination, 50.3 ug/L of HAA formed corresponding to 20.2% drop than the chlorination without PAA. Considering practical application, 50.3ug/L or a drop of 20.2% HAAs within 2 hours is acceptable and more likely to be feasible. There were no significant differences regarding THM formation potential by PAA as a function of contact time between seconds (instant) and 24 hours. The THMs formed in the samples with PAA pre-oxidation were all below the control without PAA pre-disinfection. The optimum PAA contact time for DBP control in this bench scale test is 2 hours.

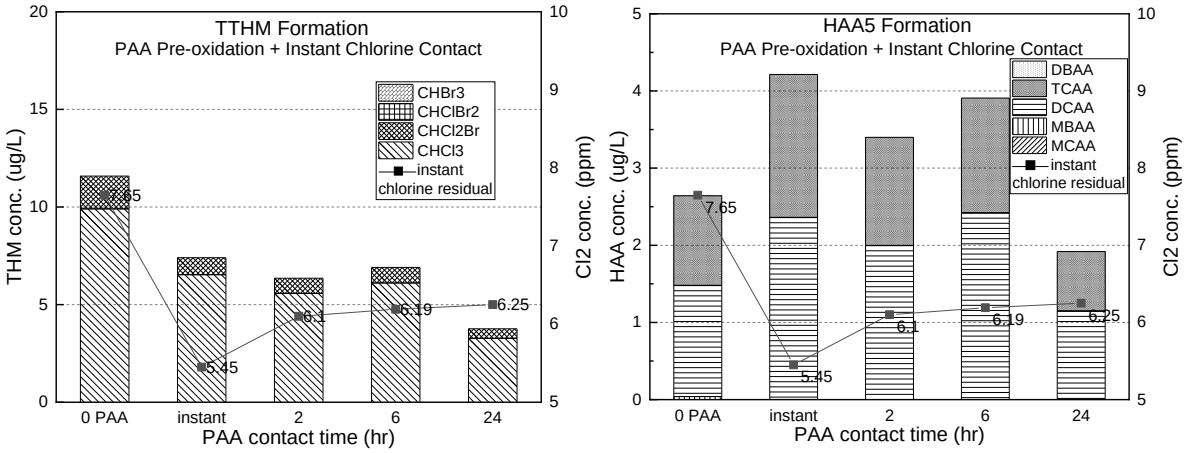

Figure 19.1 . TTHM and HAA5 Formation vs PAA Contact Time, after PAA Pre-oxidation and Chlorination, instant chlorination

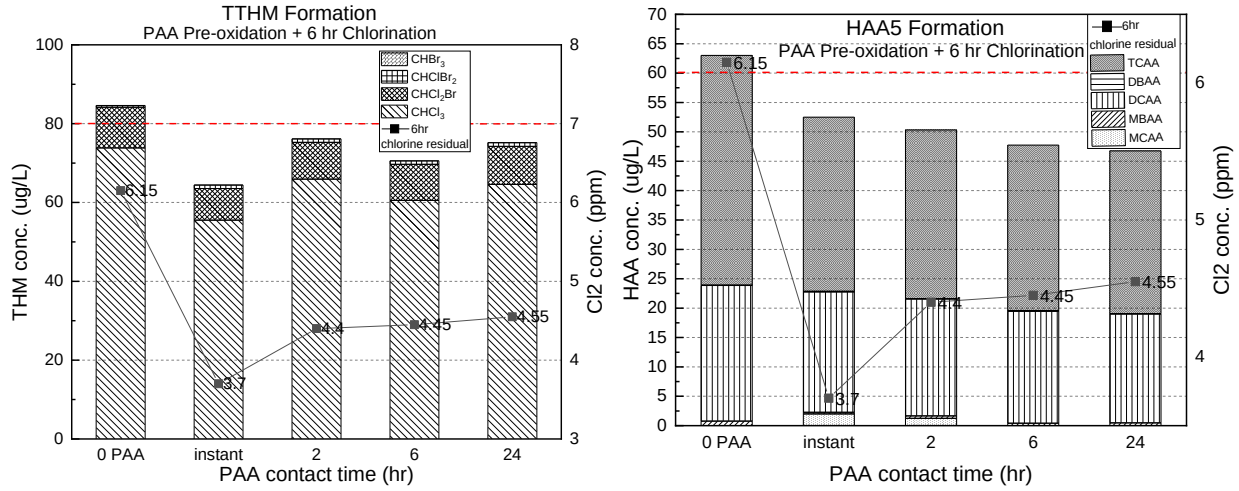

Figure 19.2 . TTHM and HAA5 Formation vs PAA Contact Time, after PAA Pre-oxidation and Chlorination, 6-hour chlorinaton

8 Conclusion

Based on studies with 2 different surface waters, PAA has been shown to destroy up to 34% of the DBP precursors (THMs and HAAs) in NOM as well as the chlorine-reactive sites on NOM. This level of precursor destruction is similar to that observed for other pre-oxidants such as ozone and chlorine dioxide. Higher PAA doses result in lower DBP formation. The fastest reacting sites (i.e., under short chlorine contact times) are destroyed to the greatest relative extent. Sunlight accelerates the decomposition of PAA in surface water. The DBP control effect of PAA pre-oxidation was greater than that of PAA decay in the dark. . Under short PAA contact times, the THM4 and HAA5 levels were

also lowered by PAA pre-oxidation. A time of 2hour was deemed sufficient to achieve substantial precursor destruction.

The PAA pre-oxidation in water treatment processes should be applied in caution. Sufficient concentration of chlorine should be dosed into the PAA pre-oxidized matrices to secure a chlorine residual in the disinfected water, since the hydrogen peroxide residual of PAA accounts for a huge part of the chlorine demand.

There are indications that the ABTS method used for determination of residual hydrogen peroxide exhibits a substantial positive bias.

9 Future Work

To test PAA effect with different waters. Establish a method to determine PAA and peroxide concentration accurately. Scale up the contact time test and find the optimum conditions in real operations. Determine downstream impacts of acetic acid residuals.

10 Reference

1. Klenk, H., et al. "Peroxy compounds, organic. Ullmann's Encyclopedia of Industrial Chemistry." (2000).
2. Tchobanoglous, G., Burton, F.L., and Stensel, H.D. (2004). Wastewater engineering treatment and reuse (pp. 1220). New York, NY: McGraw-Hill
3. Jiang Y, Goodwill JE, Tobiason JE, Reckhow DA. Comparison of ferrate and ozone pre-oxidation on disinfection byproduct formation from chlorination and chloramination. Water research. 2019 Jun 1;156:110-24.
4. Koivunen, J., Juntunen, P., and Heinonen-Tanski, H. (2005). Dissolved air flotation and peracetic acid (PAA) disinfection for treatment of municipal wastewaters. Report of the FLOTE project. University of Kuopio, Kuopio, Finland. Luukkonen, T., Heyninck, T., Ramo, J., and Lassi, U. (2015). Comparison of organic per- acids in wastewater treatment: disinfection, oxidation and corrosion. Water Res., 85, 275–285.
5. Liberti, L., and Notarnicola, M. (1999). Advanced treatment and disinfection for munici- pal wastewater reuse in agriculture. Water Sci. Technol., 40, 235–245.
6. Collivignarelli, C., Bertanza, G., and Pedrazzani, R. (2000). A comparison among different wastewater disinfection systems: Experimental results. Environ. Technol., 21, 1–16.
7. Nurizzo, C., Bonomo, L., and Malpei, F. (2001). Some economic considerations on wastewater reclamation for irrigation, with reference to the Italian situation. Water Sci. Tech- nol., 43, 75–81.
8. Koivunen, J., Juntunen, P., and Heinonen-Tanski, H. (2005). Dissolved air flotation and peracetic acid (PAA) disinfection for treatment of municipal wastewaters. Report of the FLOTE project. University of Kuopio, Kuopio, Finland.
9. Ragazzo, P., Chiucchini, N., Piccolo, V., and Ostoich, M. (2013). A new disinfection system for wastewater treatment: Performic acid full–scale trial evaluations. Water Sci. Tech- nol., 67, 2476–2487
10. Tondera, K., Klaer, K., Koch, C., Hamza, I.A., and Pinnekamp, J. (2016). Reducing patho- gens in combined sewer overflows using performic acid. Int. J. Hyg. Environ. Health, 219, 700–708.
11. Mattila, T., and Aksela, R. (2000). Method for the preparation of aqueous solutions con- taining performic acid as well as their use. U.S. Patent 6,049,002.
12. Gehr, R., Chen, D., and Moreau, M. (2009). Performic acid (PFA): Tests on an advanced primary effluent show promising disinfection performance. Water Sci. Technol., 59, 89–96.
13. Chhetri, R.K., Thornberg, D., Berner, J., Gramstad, R., Ojstedt, U., Sharma, A.K. and Andersen, H.R. (2014).

14. Chhetri, R.K., Bonnerup, A., and Andersen, H.R. (2016). Combined sewer overflow pre-treatment with chemical coagulation and a particle settler for improved peracetic acid disinfection. J. Ind. Eng. Chem., 37, 372–379.
15. Antonelli, M., Rossi, S., Mezzanotte, V., and Nurizzo, C. (2006). Secondary effluent disinfection: PAA long term efficiency. Environ. Sci. Technol., 40, 4771–4775.
16. Pedersen, L.F., Pedersen, P.B., Nielsen, J.L., and Nielsen, P.H. (2009). Peracetic acid degradation and effects on nitrification in recirculating aquaculture systems. Aquaculture, 296, 246–254.
17. Santoro, D., Gehr, R., Bartrand, T.A., Liberti, L., Notarnicola, M., Dell'Erba, A., Falsanisi, D., and Haas, C.N. (2007). Wastewater disinfection by peracetic acid: Assessment of models for tracking residual measurements and inactivation. Water Environ. Res., 79, 775–787.
18. Falsanisi, D., Gehr, R., Santoro, D., Dell'Erba, A., Notarnicola, M., and Liberti, L. (2006). Kinetics of PAA demand and its implications on disinfection of wastewaters. Water Qual. Res. J. Can., 41, 398–409.
19. Rossi, S., Antonelli, M., Mezzanotte, V., and Nurizzo, C. (2007). Peracetic acid disinfec- tion: A feasible alternative to wastewater chlorination. Water Environ. Res., 79, 341–350.
20. Cavallini, G.S., Campos, S.X.d., Souza, J.B.d., and Vidal, M.d.S. (2013). Comparison of methodologies for determination of residual peracetic acid in wastewater disinfection. Int. J. Environ. Anal. Chem., 93, 906–918.
21. Cavallini, G.S., Campos, S.X.d., Souza, J.B.d and Vidal, C.M.d.S. (2013). Evaluation of the physical-chemical characteristics of wastewater after disinfection with peracetic acid. Water Air Soil Pollut., 224, 1752–1755.
22. Dell'Erba, A., Falsanisi, D., Liberti, L., Notarnicola, M., and Santoro, D. (2004). Disinfect- ing behaviour of peracetic acid for municipal wastewater reuse. Desalination, 168, 435– 442.
23. Block, S.S. (1991). Peroxygen compounds. In S.S. Block (Ed.), Disinfection, sterilization and preservation (pp. 185–201). Philadelphia, PA: Lea & Febiger.
24. Sanz, V., De Marcos, S., and Galb?an, J. (2007). Hydrogen peroxide and peracetic acid determination in wastewater using a reversible reagentless biosensor. Anal. Chim. Acta., 583, 332–339.
25. ECHA (2015). Assessment report, peracetic acid, regulation (EU) no 528/2012 concerning the making available on the market and use ofbiocidal products, evaluation ofactive sub- stances. Finland: European Chemicals Agency.
26. Lubello, C., Caretti, C., and Gori, R. (2002). Comparison between PAA/UV and H2O2/ UV disinfection for wastewater reuse. Water Sci. Technol. Water Supply., 2, 205–212.

27. Caretti, C., and Lubello, C. (2003). Wastewater disinfection with PAA and UV combined treatment: A pilot plant study. Water Res., 37, 2365–2371.
28. Cristofari-Marquand, E., Kacel, M., Milhe, F., Magnan, A., and Lehucher–Michel, M. (2007). Asthma caused by peracetic acid-hydrogen peroxide mixture. J. Occup. Health., 49, 155–158.
29. Freer, P.C., and Novy, F.G. (1902). On the formation, decomposition and germicidal action of benzoylacetyl and diacetyl peroxides. Am. Chem. J., 27, 6–92.
30. West, D.M., Wu, Q., Donovan, A., Shi, H., Ma, Y., Jiang, H., and Wang, J. (2016). N-nitrosamine formation by monochloramine, free chlorine, and peracetic acid disinfection with presence of amine precursors in drinking water system. Chemosphere, 153, 521–527.
31. Yuan, Z., Ni, Y., and Van Heiningen, A. (1997). Kinetics of peracetic acid decomposition: Part I: Spontaneous decomposition at typical pulp bleaching conditions. Can. J. Chem. Eng., 75, 37–41.
32. Yuan, Z., Ni, Y., and Van Heiningen, A. (1997). Kinetics of the peracetic acid decomposi- tion: Part II: pH effect and alkaline hydrolysis. Can. J. Chem. Eng., 75, 42–47.
33. Monarca, S., Zani, C., Richardson, S.D., Thruston, A.D., Moretti, M., Feretti, D., and Vil- larini, M. (2004). A new approach to evaluating the toxicity and genotoxicity of disin- fected drinking water. Water Res., 38, 3809–3819.
34. Bianchini, R., Calucci, L., Lubello, C., and Pinzino, C. (2002). Intermediate free radicals in the oxidation of wastewaters. Res. Chem. Intermediat., 28, 247–256.
35. Bianchini, R., Calucci, L., Caretti, C., Lubello, C., Pinzino, C., and Piscicelli, M. (2002). An EPR study on wastewater disinfection by peracetic acid, hydrogen peroxide and UV irradiation.
36. Dell'Erba, A., Falsanisi, D., Liberti, L., Notarnicola, M., and Santoro, D. (2007). Disinfec- tion by-products formation during wastewater disinfection with peracetic acid. Desalina- tion, 215, 177–186.
37. Crebelli, R., Conti, L., Monarca, S., Feretti, D., Zerbini, I., Zani, C., Veschetti, E., Cutilli, D., and Ottaviani, M. (2005). Genotoxicity of the disinfection by–products resulting from peracetic acid- or hypochlorite-disinfected sewage wastewater. Water Res., 39, 1105–1113.
38. Zhou, F., Lu, C., Yao, Y., Sun, L., Gong, F., Li, D., Pei, K., Lu, W., and Chen, W. (2015). Activated carbon fibers as an effective metal-free catalyst for peracetic acid activation: Implications for the removal of organic pollutants. Chem. Eng. J., 281, 953–960.
39. Rokhina, E.V., Makarova, K., Lahtinen, M., Golovina, E.A., Van As, H., and Virkutyte, J. (2013). Ultrasound–assisted MnO2 catalyzed homolysis of peracetic acid for phenol deg- radation: The assessment of process chemistry and kinetics. Chem. Eng. J., 221, 476–486.

40. Zhao, X., Zhang, T., Zhou, Y., and Liu, D. (2007). Preparation of peracetic acid from hydrogen peroxide: Part I: Kinetics for peracetic acid synthesis and hydrolysis. J. Mol. Catal. A: Chem., 271, 246–252
41. Zhao, X., Cheng, K., Hao, J., and Liu, D. (2008). Preparation of peracetic acid from hydrogen peroxide, Part II: kinetics for spontaneous decomposition of peracetic acid in the liquid phase. J. Mol. Catal. A: Chem., 284, 58–68.
42. Zhang, W., Cao, B., Wang, D., Ma, T., Xia, H., and Yu, D. (2016). Influence of wastewater sludge treatment using combined peroxyacetic acid oxidation and inorganic coagulants re-flocculation on characteristics of extracellular polymeric substances (EPS). Water Res., 88, 728–739.
43. Zhang, X.Z., Francis, R.C., Dutton, D.B., and Hill, R.T. (1998). Decomposition of perace- tic acid catalyzed by Cobalt (II) and Vanadium(V). Can. J. Chem., 76, 1064–1069.
44. Kitis, M. (2004). Disinfection of wastewater with peracetic acid: A review. Environ. Int., 30, 47–55.
45. Wagner, M., Brumelis, D., and Gehr, R. (2002). Disinfection of wastewater by hydrogen peroxide or peracetic acid: Development of procedures for measurement of residual dis- infectant and application to a physicochemically treated municipal effluent. Water Envi- ron. Res., 74, 33–50.
46. Caretti, C., and Lubello, C. (2003). Wastewater disinfection with PAA and UV combined treatment: A pilot plant study. Water Res., 37, 2365–2371.
47. Chen, J., Pavlostathis, S.G., 2019. Peracetic acid fate and decomposition in poultry processing wastewater streams. Bioresour. Technol. Rep. 7, 100285.
48. Carey, F.A., 2011. Química Organica, vol. 2. Mc Graw Hill. 7 ediçao.
49. Henao, L.D., Compagni, R.D., Turolla, A., Antonelli, M., 2018. Influence of inorganic and organic compounds on the decay of peracetic acid in wastewater disinfection. Chem. Eng. J. 337, 133-142.
50. Bianchini, R., Calucci, L., Lubello, C., Pinzino, C., 2002. Intermediate free radicals in the oxidation of wastewaters. Res. Chem. Intermed. 28 (2-3), 247-256.
51. Cai, M., Sun, P., Zhang, L., Huang, C., 2017. UV/Peracetic acid for degradation of pharmaceuticals and reactive species evaluation. Environ. Sci. Technol. 51 (24), 14217-14224.
52. Macedo, L.P.R., Dornelas, A.S.P., Vieira, M.M., Ferreira, J.S.J., Sarmento, R.A., Cavallini, G.S., 2019. Comparative ecotoxicological evaluation of peracetic acid and the active chlorine of calcium hypochlorite: use of Dugesia tigrina as a bioindicator of environmental pollution. Chemosphere 233, 273-281.

53. Xue, R., Shi, H., Ma, Y., Yang, J., Hua, B., Inniss, E.C., Adams, C.D., Eichholz, T., 2017. Evaluation of thirteen haloacetic acids and ten trihalomethanes formation by peracetic acid and chlorine drinking water disinfection. Chemosphere 189, 349-356.
54. Zhang, C., Brownb, P.J.B., Hu, Z., 2018. Thermodynamic properties of an emerging chemical disinfectant, peracetic acid. Sci. Total Environ. 621, 948-959.
55. Manoli, K., Sarathy, S., Maffettone, R., Santoro, D., 2019. Detailed modeling and advanced control for chemical disinfection of secondary effluent wastewater by peracetic acid. Water Res. 153, 251-262.
56. Du, P., Liu, W., Cao, H., Zhao, H., Huang, C.H., 2018. Oxidation of amino acids by peracetic acid: reaction kinetics, pathways and theoretical calculations. Water Res. X 1, 100002.
57. Wang CX, Zhang WJ, Wang DS and Wang QF, Enhancement of activated sludge dewatering performance with combined peroxyacetic acid and ferrous iron. Chin J Environ Eng 9:3975–3984 (2015) (in Chinese).
58. Sun DD, Qiao MY, Xu YY, Ma C and Zhang XX, Pretreatment of waste activated sludge by peracetic acid oxidation for enhanced anaerobic digestion. Environ Prog Sustain Energy 37:2058–2062 (2018).
59. Hollman, J., Dominic, J. A. and Achari, G. (2020) 'Degradation of pharmaceutical mixtures in aqueous solutions using UV/peracetic acid process: Kinetics, degradation pathways and comparison with UV/H2O2', Chemosphere. Elsevier Ltd, 248, p. 125911. doi: 10.1016/j.chemosphere.2020.125911.
60. Kim, J. et al. (2019) 'Advanced Oxidation Process with Peracetic Acid and Fe(II) for Contaminant Degradation', Environmental Science and Technology, 53(22), pp. 13312–13322. doi: 10.1021/acs.est.9b02991.
61. da Silva, W. P. et al. (2020) 'Peracetic acid: Structural elucidation for applications in wastewater treatment', Water Research. Elsevier Ltd, 168, p. 115143. doi: 10.1016/j.watres.2019.115143.
62. Sully, B. Y. B. D. and Williams, P. L. (no date) 'Analysis of Solutions of Per-acids and', October, pp. 653–657.
63. Zhang, T. and Huang, C. H. (2020) 'Simultaneous quantification of peracetic acid and hydrogen peroxide in different water matrices using HPLC-UV', Chemosphere. Elsevier Ltd, 257, p. 127229. doi: 10.1016/j.chemosphere.2020.127229.
64. Wang, J. et al. (2020) 'A novel and effective pretreatment to stimulate short-chain fatty acid production from waste activated sludge anaerobic fermentation by ferrous iron catalyzed peracetic acid', Journal of Chemical Technology and Biotechnology, 95(3), pp. 567–576. doi: 10.1002/jctb.6232.

65. Rizzo, L. et al. (2018) ‘Antibiotic contaminated water treated by photo driven advanced oxidation processes: Ultraviolet/H2O2 vs ultraviolet/peracetic acid’, Journal of Cleaner Production. Elsevier Ltd, 205, pp. 67–75. doi: 10.1016/j.jclepro.2018.09.101.
66. Rizzo, L. et al. (2019) ‘Tertiary treatment of urban wastewater by solar and UV-C driven advanced oxidation with peracetic acid: Effect on contaminants of emerging concern and antibiotic resistance’, Water Research, 149, pp. 272–281. doi: 10.1016/j.watres.2018.11.031.

Appendix

A. Determination of Peracetic Acid (PAA) in Water by HACH DPD Method

Equipment and Reagents:

MR and HR Chlorine Pocket Colorimeter (PCII) – Hach PN 5870062 (Use HR program)

10-mL/1-cm Sample Cell – Hach PN 4864302

DPD Total Chlorine Reagent Powder Pillow, 25-mL, 100/pkg – Hach PN 1406499; (Do Not use Free DPD Reagents)

Ammonium Molybdate 100-mL Dropper Bottle – Hach PN 193332

Test Procedure for PAA:

When using the PCII, make sure that the program is in the HR mode, use program 12 for the DR800 series colorimeters, and for all other Hach colorimeters and spectrophotometers use program 88 for HR Total Chlorine, Hach Method 10070.

(1) Fill both 10 mL sample cells with the water sample. One of these cells will be the blank and the other will be the prepared sample.

(2) Place the blank into the instrument and press the 'zero' key.

(3) Add the contents of one DPD TOTAL 25-mL Chlorine powder pillow to the prepared sample cell.

(4) Cap the prepared sample cell and shake gently to mix the DPD powder. A pink color will develop indicating the presence of PAA.

(5) After 15 to 20 seconds after adding the DPD powder to the prepared sample cell, ensure that the DPD powder has dissolved and there are no air bubbles present (invert lightly to dislodge the air bubbles), use a lab wipe to clean off the 10-mL/1-cm cell. Between 45 and 60 seconds of reaction time, place the sample cell into the cell compartment and then press 'read'. Do not wait more than 60 seconds to read the sample.

(6) The results are in mg/L as total Cl2. Convert the mg/L Cl2 value to mg/L of PAA by multiplying the value by 1.07. If you instrument has the built in dilution factor function, you can input the 1.07 with this option.

$$\text{mg/L PAA} = 1.07 \times \text{mg/L Total Cl2 PAA}$$

B. Determination of Hydrogen Peroxide by ABTS UV Absorbance Method – UMass

1. Solution preparation.

a. Horseradish peroxidase (HRP) stock solution: 50 mg/L. 25 mL in total. Spike 1.25 mg of HRP from brown bottle into 25 mL of Mili-Q water and mix. The HRP solid can be found in freezer in

Room 308. It should be noted that HRP has a very short half-life. The HRP stock solution **has to be remade daily** if needed.

b. Phosphate buffer: The buffer used in this method is at pH = 7.0. Using balance in Room 308 to measure out 1.09 gram of Na2HPO4 and 1.70 gram of NaH2PO4-H2O. Dissolve both chemicals into 200 mL of Mili-Q water.

c. ABTS stock solution: 1 g/L. Total volume is 25 mL. Spike 25 mg of ABTS into 25 mL of Mili-Q water and mix. The ABTS has a relatively short half-life. It is strongly recommended that this ABTS stock solution has to be remade every month.

2. Operation procedure.

a. Prepare a clean 25 mL volumetric bottle. This bottle will be used as the prime container for the following spiking and mixing steps.

b. Add 3 mL of phosphate buffer solution into the 25 mL volumetric bottle.

c. Add 1 mL of ABTS stock solution into the 25 mL volumetric bottle.

d. Add 1 mL of HRP stock solution into the 25 mL volumetric bottle.

f. Add 0.5 mL to 2 mL of hydrogen peroxide sample into the 25 mL volumetric bottle. The mixed solution should turns into dark green/blue color from light green color, which suggests the existence hydrogen peroxide. Gently shake the bottle.

g. Fill the 25 mL volumetric bottle to the mark using Mili-Q water. Mix thoroughly. Wait for 5 minutes until the reaction is finished.

h. Check the UV-absorbance at 415 nm.

3. Calculation.

The reaction between ABTS and hydrogen peroxide produces ABTS+ which gives dark green/blue color in water. The molar ratio between consumed hydrogen peroxide and produced ABTS+ is 1:2. ABTS+ has one distinguishable peak at 415 nm (ε=36000 M-1*cm-1). Then the calculation for hydrogen peroxide can be summarized as follow:

$$c\left(H_2O_2\ \left(\frac{\text{mg}}{\text{L}}\right)\right) = \frac{\Delta Abs\ (cm^{-1})\ \times V_{Total}\ (mL)}{\varepsilon\ (M^{-1}cm^{-1}) \times V_S\ (mL)} \times 0.5\ \times 34000\ \frac{mg}{mol}$$

ΔAbs - UV-absorbance difference at 415 nm. V_{Total} - Total volume, usually is 25 mL.

ε - The molar absorbance of ABTS+ at 415 nm, 36000 M-1/cm-1. V_s - Sample volume, 0.5 - 2.0 mL.

C. UMass Chlorination Procedure:

http://www.ecs.umass.edu/eve/research/sop/Chlorination.pdf?_ga=2.202287826.2106045631.1584084772-1924450244.1528301788

D. UMass THM Extraction Procedure:

http://www.ecs.umass.edu/eve/research/sop/THM.pdf?_ga=2.202287826.2106045631.1584084772-1924450244.1528301788

E. UMass HAA Extraction Procedure:

http://www.ecs.umass.edu/eve/research/sop/HAA.pdf?_ga=2.202287826.2106045631.1584084772-1924450244.1528301788

F. Weather During PAA Sunlight Decay Test

Amherst, MA Hourly Weather

12:08 pm EDT

TIME	DESCRIPTION	TEMP	FEELS	PRECIP	HUMIDITY	WIND
12:15 PM TUE	Sunny/Wind	63°	60°	0%	38%	NW 20 mph
1:00 PM TUE	Sunny/Wind	64°	61°	0%	36%	NW 20 mph
2:00 PM TUE	Sunny/Wind	65°	63°	0%	34%	NW 20 mph
3:00 PM TUE	Sunny/Wind	66°	66°	0%	32%	NW 21 mph
4:00 PM TUE	Sunny	65°	63°	0%	34%	NW 19 mph
5:00 PM TUE	Sunny	65°	63°	0%	34%	NW 19 mph
6:00 PM TUE	Sunny	64°	62°	0%	34%	NW 17 mph
7:00 PM TUE	Sunny	62°	60°	0%	37%	NW 15 mph
8:00 PM TUE	Sunny	59°	57°	0%	43%	NW 11 mph
9:00 PM TUE	Clear	57°	55°	0%	47%	NW 8 mph
10:00 PM TUE	Clear	55°	53°	0%	48%	NW 8 mph
11:00 PM TUE	Clear	54°	52°	0%	50%	NW 8 mph
12:00 AM WED	Clear	53°	51°	0%	52%	NW 7 mph

Amherst, MA Hourly Weather

11:13 am EDT

TIME	DESCRIPTION	TEMP	FEELS	PRECIP	HUMIDITY	WIND
11:30 AM WED	Mostly Sunny	66°	66°	0%	32%	N 13 mph
12:00 PM WED	Mostly Sunny	67°	67°	0%	31%	N 13 mph
1:00 PM WED	Sunny	69°	69°	0%	29%	NNW 11 mph
2:00 PM WED	Sunny	70°	70°	0%	28%	NNW 10 mph
3:00 PM WED	Sunny	71°	71°	0%	29%	NNW 8 mph
4:00 PM WED	Sunny	72°	72°	0%	28%	NNW 8 mph
5:00 PM WED	Mostly Sunny	72°	72°	0%	28%	NNW 7 mph
6:00 PM WED	Mostly Sunny	71°	71°	0%	31%	N 6 mph
7:00 PM WED	Mostly Sunny	69°	69°	0%	38%	N 4 mph
8:00 PM WED	Sunny	64°	64°	0%	45%	NNE 3 mph
9:00 PM WED	Mostly Clear	60°	60°	0%	54%	NE 2 mph